universität wien

MASTERARBEIT / MASTER'S THESIS

Titel der Masterarbeit / Title of the Master's Thesis

„The role of ELF5 in human trophoblast stem cells“

verfasst von / submitted by

Astrid Guth, BSc

angestrebter akademischer Grad / in partial fulfilment of the requirements for the degree of

Master of Science (MSc)

Wien, 2022 / Vienna, 2022

Studienkennzahl lt. Studienblatt / degree programme code as it appears on the student record sheet:	UA 066 877
Studienrichtung lt. Studienblatt / degree programme as it appears on the student record sheet:	Masterstudium Genetik und Entwicklungsbiologie
Betreut von / Supervisor:	Dr. Paulina Latos

Acknowledgements

I would like to thank Dr. Paulina Latos for her incredible guidance and support throughout this project. I am also very grateful for the kindness of the other lab members, in particular Ruth Hornbachner and Delyana Stoeva, who provided invaluable help and advice when it came to performing the experiments.

Table of Contents

1. Abstract

The placenta plays an essential role in pregnancy and embryonic development by providing a site of exchange for nutrients, gases and metabolites between the mother and the embryo. This interface is established during the development of the placenta in the first trimester, which is mediated by the proliferation and differentiation of multipotent trophoblast progenitor cells called cytotrophoblasts (CTBs). CTBs give rise to two main subtypes, extravillous trophoblasts and syncytiotrophoblasts, and failures in these differentiation pathways can lead to various placental pathologies. The underlying transcriptional regulation of trophoblast differentiation in humans remains poorly understood, in part due to a lack of accurate and reliable model systems. Therefore, the recent establishment of human trophoblast stem cells (hTSCs) that faithfully recapitulate the differentiation potential of their *in vivo* counterparts was a breakthrough in the field.

Here, I explore the role of the transcription factor E74-like ETS transcription factor 5 (ELF5) in regulating the self-renewal and commitment of hTSCs. Since murine Elf5 acts as a master regulator of trophoblast fate, and human *ELF5* expression is restricted to CTBs, I hypothesize that precise levels of this factor are required for proper differentiation. I investigate this by generating knock-down and overexpression cell lines, and analysing them by microscopy, qPCR and immunofluorescence. Surprisingly, the results show that hTSC are not significantly impaired by disrupted ELF5 levels, suggesting that ELF5 has a different function in humans than in mice. Alternatively, I propose that ELF5 levels could relate to the developmental stage of the placenta, and that hTSCs correspond to a later timepoint at which its expression is decreased. To open further investigations into this, I generate a ELF5-V5 tagged cell line for functional analysis, and a ELF5-EYFP reporter cell line for a direct readout of *ELF5* expression.

Overall, the experiments described here provide additional molecular insights into human placentation and highlight the need for a more optimized model system when investigating placental disorders.

Zusammenfassung

Die Plazenta spielt eine wesentliche Rolle in der Schwangerschaft und der embryonalen Entwicklung, da sie eine Schnittstelle für den Austausch von Nährstoffen, Gasen und Stoffwechselprodukten zwischen der Mutter und dem Embryo darstellt. Diese Verbindung wird während der Entwicklung der Plazenta im ersten Trimester durch die Proliferation und Differenzierung von multipotenten Trophoblastenvorläuferzellen, den sogenannten Cytotrophoblasten (CTBs), hergestellt. Aus den CTBs entstehen zwei Hauptuntertypen, extravillöse Trophoblasten und Synzytiotrophoblasten. Störungen in diesen Differenzierungswegen können zu verschiedenen Plazenta-Pathologien führen. Die zugrundeliegende Transkriptionsregulation der Trophoblastendifferenzierung beim Menschen ist nur unzureichend erforscht, was zum Teil daran liegt, dass es keine genauen und zuverlässigen Modellsysteme gibt. Daher war die kürzliche Herstellung von humanen Trophoblastenstammzellen (hTSCs), die das Differenzierungspotenzial ihrer in vivo-Gegenstücke getreu rekapitulieren, ein Durchbruch in diesem Bereich.

Hier untersuche ich die Rolle des E74-like ETS-Transkriptionsfaktors 5 (ELF5) bei der Regulierung der Selbsterneuerung und des Commitments von hTSCs. Da Elf5 in der Maus als Hauptregulator des Trophoblastenschicksals wirkt und die humane ELF5-Expression auf die CTBs beschränkt ist, stelle ich die Hypothese auf, dass spezifische Expression dieses Faktors für die richtige Differenzierung erforderlich ist. Ich untersuche dies durch die Herstellung von Knockdown- und Überexpressions-Zelllinien und analysiere sie mittels Mikroskopie, qPCR und Immunfluoreszenz. Überraschenderweise zeigen die Ergebnisse, dass hTSC durch gestörte ELF5-Expression nicht signifikant beeinträchtigt werden, was darauf hindeutet, dass ELF5 beim Menschen eine andere Funktion hat, als bei Mäusen. Alternativ schlage ich die These auf, dass die ELF5-Expression mit dem Entwicklungsstadium der Plazenta zusammenhängen könnte und dass hTSCs einen späteren Zeitpunkt repräsentieren, an Welchem diese verringert ist. Um dies weiter

zu untersuchen, entwickle ich eine ELF5-V5 getaggte Zelllinie für funktionelle Analysen und eine ELF5-EYFP-Reporterzelllinie für eine direkte Messung der ELF5-Expression.

Insgesamt bieten die hier beschriebenen Experimente zusätzliche molekulare Einblicke in die menschliche Plazentation und unterstreichen den Bedarf an einem optimierten Modellsystem für die Untersuchung von Plazentaerkrankungen.

2. Abbreviations

µl	Microliter
µM	Micromolar
APS	Ammonium persulfate
bp	Basepairs
BMP	Bone morphogenic protein
BSA	Bovine serum albumin
cAMP	Cyclic adenosine monophosphate
cDNA	Complementary deoxyribonucleic acid
CDS	Coding sequence
CDX2	Caudal type homeobox 2
CGA	Glycoprotein hormones alpha chain
CGB	Chorionic gonadotropin beta
ChIP	Chromatin immunoprecipitation
CHIR99021	Glycogen synthase kinase-3 inhibitor
CT	Cytotrophoblast
DAPI	4',6-Diamidin-2-phenylindol
dNTP	Deoxyribonucleoside triphosphate
Dox	Doxycycline
DTT	Dithiothreitol
EDTA	Ethylenediamine tetraacetic acid
EMT	Epithelial to mesenchymal transition
EVT	Extravillous trophoblast
EGF	Epidermal growth factor
ELF5	E74 like ETS transcription factor 5
ENDOU	Poly(U)-specific endoribonuclease
EOMES	Eomesodermin
ERVW-1	Endogenous retrovirus group W member 1
ESC	Embryonic stem cell
ESRRB	Estrogen related receptor gene
EtOH	Ethanol
EYFP	Enhanced yellow fluorescent protein
FGF4	Fibroblast growth factor 4
GATA2/3	GATA-binding protein 2/3
GCM1	Glial cell missing homolog 1
hPSC	Human pluripotent stem cell

iOX	Inducible overexpression
kb	Kilobase
KD	Knockdown
KRT7	Keratin 7
$MgCl_2$	Magnesium chloride
mM	Millimolar
mRNA	Messenger ribonucleic acid
mSA	Maternal spiral arteries
NaCl	Sodium chloride
NeoR	Neomycin (G418) resistance gene
NP40	Nonidet P 40
OX	Overexpression
PBGD	Hydroxymethylbilane synthase
PBS	Phosphate buffered saline
PCR	Polymerase chain reaction
PMSF	Phenylmethylsulfonyl fluoride
RNA	Ribonucleic acid
RT-qPCR	Quantitative reverse transcription PCR
SDC1	Syndecan 1
SDS	Sodium dodecyl sulfate
SEM	Standard error of the mean
shRNA	Short hairpin RNA
SR	Self-renewal
ST	Syncytiotrophoblast
TB-ORG	Trophoblast organoid
TE	Trophectoderm
TEAD4	TEA domain transcription factor 4
TEMED	Tetramethylethylenediamine
TGF-β	Transforming growth factor β
TF	Transcription factor
TP63	Tumor protein 63
Tris	Tris(hydroxymethyl)aminomethane
TSC	Trophoblast stem cell
vCTB	Villous cytotrophoblast
Y27632	Rho-associated protein kinase inhibitor

3. Introduction

3.1. The role of the human placenta

The placenta is a transient organ that connects the developing embryo to the mother during gestation and mediates the exchange of nutrients, gases, and waste (Hemberger et al., 2019). It is also an endocrine organ that produces important hormones throughout gestation, both for its proper development and for the alteration of maternal physiology during pregnancy (Napso et al., 2018). Thus, it plays an essential and central role in mammalian embryogenesis.

Placentation is defective in 1 out of 10 pregnancies, leading to various disorders such as intrauterine growth restriction, preeclampsia, miscarriage, recurrent abortion, and preterm labor (Brosens et al., 2011). These abnormal placentation events have a significant long-term impact on the health of both the fetus and the mother, making them responsible for a high proportion of maternal and neonatal morbidity (Graham et al., 2016). Although defects in placental function usually manifest in the second or third trimester, the underlying causes of these disorders occur in the earlier stages of pregnancy (Smith, 2010). The establishment of the feto-maternal interface upon implantation of the blastocyst followed by the rapid development of the placenta during the first few weeks of gestation is critical. During this time, trophoblast progenitor cells generate distinct differentiated cell types with various functions. These include immunological acceptance, the physiological adaptation of the mother, vascular connection to the maternal circulation and nutrition of the developing embryo. The invasion and remodeling of maternal arteries by trophoblast cells is particularly important, and when insufficient it has been defined as the ultimate cause of many pregnancy disorders (Turco et al., 2019).

Although the importance of correct specification and functionality of distinct trophoblast subtypes in early development is known, there remains much to be understood about the underlying molecular mechanisms responsible, especially in the transcriptional program.

3.2. The development of the human placenta

The development of the placenta during the first trimester involves a series of cell fate decisions and tissue specification events, starting with the first lineage segregation between the trophectoderm (TE) and the inner cell mass (ICM) of the pre-implantation blastocyst, which occurs around day 5-6 post-fertilization (E5-6) in humans. The cells of the ICM give rise to the epiblast (EPI) and primitive endoderm (PE) which will later form the embryo proper and extraembryonic tissue, respectively (Niakan et al., 2012). The cells of the TE, on the other hand, mediate blastocyst implantation around E6-7 and are the precursors of all trophoblast cells of the placenta (Turco et al., 2019). The TE is determined by the expression of the transcription factor CDX2, while the ICM is determined by the expression of the pluripotency transcription factors NANOG and OCT4. While in the mouse, Cdx2 and Oct4 are mutually exclusive, human OCT4 becomes restricted to the ICM just prior to implantation and is therefore initially coincident with CDX2 (Niakan and Eggan, 2013).

The early post-implantation developmental stages of the trophoblast lineage are mainly based on morphological studies due to the limited accessibility of human material for molecular investigations (Knöfler et al., 2001). Placental development begins at E8, during which the cells of the TE start to form a continuously expanding extraembryonic trophoblastic shell, while the ICM undergoes embryonic development. At this stage, the two main trophoblast lineages are proliferative cytotrophoblasts (CTBs) and primitive syncytium, formed by the fusion of CTBs and composed of syncytiotrophoblasts (STs) (Fig. 1). At E9, vacuoles start to appear in the syncytium, which upon fusion form lacunar spaces, further merging to become lacunar networks at E12-13, and eventually breaching the maternal uterine capillaries and forming discontinuous maternal blood sinusoids. Simultaneously, the extra embryonic mesoderm (ExM) lineage develops, presumably from cells of the PE (Fig. 1) (Knöfler et al., 2019).

Placental villi, or chorionic villi, are the structures of the placenta responsible for providing maximal contact with maternal blood. The development of chorionic villi begins at E10, as proliferative CTBs break through the expanding syncytium and extend into the maternal decidua to form primary chorionic villi (Fig. 1). These primary villi are first transformed into secondary villi by the incoming migration of ExM cells, and then into tertiary villi by the differentiation of these ExM cells into placental vessels by E17 (Knöfler et al., 2019). In the meantime, villous trees form by continuous branching, and the lacunae become the intervillous space, which is filled with maternal blood. Therefore, the early first semester developing embryo is surrounded by three layers: the inner chorionic plate, the villous placenta (villi separated by the intervillous space), and the CTB shell which is in contact with the maternal decidua (Turco et al., 2019).

Mature chorionic villi can be classified into two types – anchoring villi, which anchor to maternal tissue, and floating villi, which float in the maternal blood of the intervillous space (Fig. 2). During the final stages of placental development in the late first and second trimesters, the placental vasculature continues to undergo extensive expansion, eventually pushing up the placental capillaries against the syncytium layer of chorionic villi and maximising the area for exchange (Knöfler et al., 2019). This formation of the feto-maternal interface in humans is classified as haemochorial placentation. In contrast to the placentation of some other mammals, haemochorial placentation is characterized by invasive trophoblast cells that infiltrate the maternal uterine blood vessels and release blood into the intervillous space, thereby surrounding the outer ST layer of the chorionic villi with maternal blood (Fig. 2) (Moffett and Locke, 2006).

Overall, proliferating undifferentiated CTB progenitor cells are the driving force behind the development of chorionic villi. The CTB pool self-replenishes while also differentiating to adopt distinct cell fates, thus getting gradually exhausted during placental development (Knöfler et al., 2001).

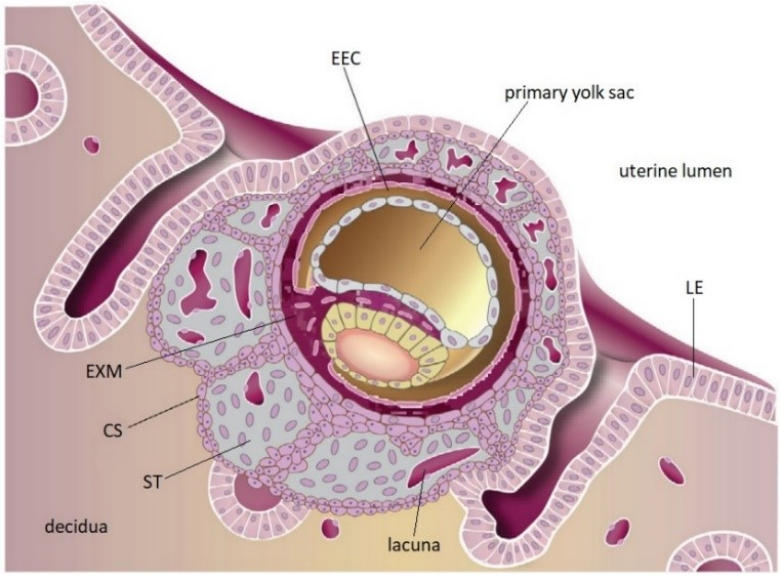

Figure 1. The primary villous stage of early human placenta development (E8-E10).
EEC, extra embryonic coelem; ExM, extra embryonic mesoderm: CS, cytotrophoblastic shell; ST, syncytiotrophoblast; LE, luminal epithelium. *Adapted from Turco et al., 2019.*

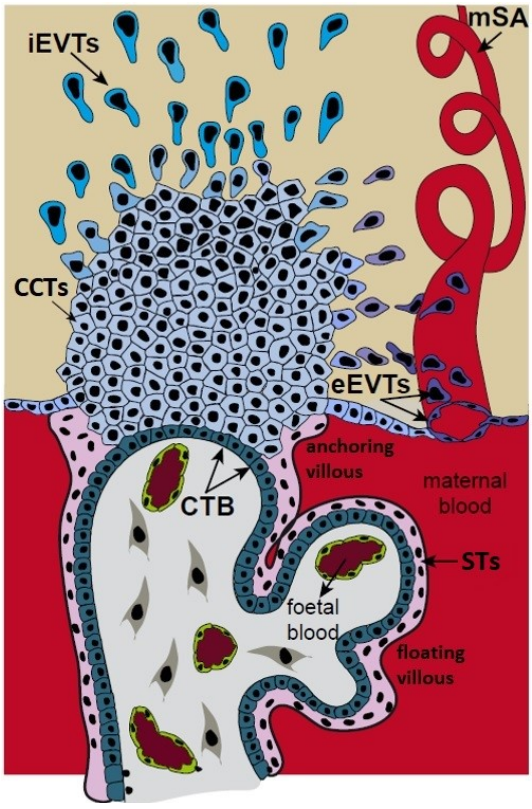

Figure 2. Structure of anchoring and floating chorionic villi.
Depending on their location, proliferative CTBs give rise to the ST layer and to EVTs. iEVTs infiltrate the decidua and eEVTs colonize mSAs. Besides trophoblasts, chorionic villi also contain stromal cells and placental endothelial cells which originate from the ExM. CTB, cytotrophoblast; STs, syncytiotrophoblasts; iEVTs, interstitial extravillous trophoblasts; eEVTs, endovascular extravillous trophoblasts; mSA, maternal spiral artery. *Adapted from Knöfler et al., 2013*

3.3. Trophoblast cell types

Proliferating CTBs are characterised by the expression of key factors required for self-renewal and stemness, in particular the following transcription factors: TEA domain transcription factor 4 (*TEAD4*), GATA-binding protein 3 (*GATA3*), transcription factor AP-2 gamma (*TFAP2C*), tumour protein 63 (*TP63*), msh homeobox 2 (*MSX2*) and E74-like ETS transcription factor 5 (*ELF5*). These factors specify early trophoblast progenitor identity and inhibit differentiation (Saha et al., 2020, Paul et al., 2017, Kuckenberg er al., 2012, Li et al., 2014, Hornbachner et al., 2021, Hemberger et al., 2010). CTBs can also downregulate their expression and exit self-renewal to adopt two distinct differentiation pathways.

The first of these differentiation pathways is fusion to form multinucleated syncytiotrophoblasts (STs), which envelop the chorionic villi and cover the surface of the developing placenta (Fig. 2). STs constitute the interface between maternal and fetal blood, and transport nutrients between the two circulations. They are also responsible for producing placental hormones such as chorionic gonadotrophin (hCG), placental lactogens (hPL) and placental growth hormone (Napso et al., 2018). The multinucleated structure of STs and lack of cell borders is likely important for facilitating diffusion between bloodstreams, and they are additionally covered in microvilli to increase the surface area for exchange (Teasdale and Jean-Jacques, 1985). Another function of STs is to act as a protective immunological barrier, both by protecting the fetus from maternal pathogens, and by not expressing human leukocyte antigen (HLA) so that maternal immune cells will not detect them as non-self (Moffett and Locke, 2006).

The transition from CTB to ST is characterised by an upregulation of ST-specific markers, which include the previously mentioned hormones hCG (encoded by the genes *CGA* and *CGB*) and hPL (encoded by the gene *CSH1*) (Napso et al., 2018). Furthermore, differentiation to ST is reinforced by a feedback loop in which hCG binds to receptors on CTBs and, through cAMP signalling, causes the activation of glial cell missing 1 (*GCM1*). GCM1 is a transcription factor that controls ST

differentiation through the upregulation of its target genes, including genes that encode the fusogenic proteins syncytin-1 and -2 and placental growth factor (Cheong et al., 2015). Another key marker protein is syndecan-1 (encoded by the gene *SDC1*), a surface heparan sulphate proteoglycan which binds to the extracellular matrix and mediates interaction between the placenta and the maternal decidua (Jokimaa et al., 1998).

The second differentiation pathway of CTBs is to extravillous trophoblasts (EVTs) which arise at the tips of anchoring villi, at the interface between fetal and maternal tissue (i.e. where the CTB shell is in contact with the decidua) (Fig. 2). CTBs first differentiate into EVT progenitors called proximal cell column trophoblasts (pCCTs) which form cell columns and then differentiate into distal cell column trophoblasts (dCCTs) (Pollheimer et al., 2018). While pCCTs are still proliferative, dCCTs cease to proliferate and dissociate from the column. They subsequently differentiate further into two distinct non-dividing EVT populations, migratory endovascular EVTs (eEVTs) and invasive interstitial EVTs (iEVTs) (Fig. 2). iEVTs invade the maternal decidua and the first third of the myometrium, after which they fuse into multinucleated trophoblast giant cells that lose invasive capacity and produce pregnancy-specific hormones such as hPL and hCG. eEVTs, on the other hand, replace the endothelial cells of the maternal spiral arteries (mSAs), transforming them into wide, low resistance channels and thereby increasing blood flow. Remarkably, during the first 6 weeks of pregnancy eEVTs initially form trophoblast plugs that prevent blood flow from the SAs, resulting in a low oxygen environment thought to be key for placenta development, vasculogenesis and angiogenesis (Weiss et al., 2016). iEVTs contribute to the subsequent loss of mSA vasoactivity by interacting with maternal immune cells, so overall the combined effect of both types of EVTs is a remodeling of mSAs, which is crucial for facilitating greater nutrient uptake by the growing fetus (Velicky et al., 2015). Disruption to the control and homeaostasis of EVT invasion has been shown to specifically contribute to several placental pathologies such as early onset preeclampsia (Davies et al., 2016),

and incomplete mSA plugging by eEVTs was seen in miscarried pregnancies (Weiss et al., 2016).

The progressive differentiation from CTBs to EVTs involves epithelial to mesenchymal transition (EMT), as immotile, polarized cells adopt mesenchymal characteristics including the ability to migrate (Davies et al., 2016). The uterine environment controls this EMT very tightly and NOTCH1 has been identified as the key regulator promoting the early development of CCTs (Haider et al., 2016). Along with the downregulation of epithelial markers and upregulation of endothelial markers, EVT identity is defined by the upregulation of various other genes involved in growth, cell adhesion and cell motility. These include human leukocyte antigen G (*HLA-G*), a class I major histocompatibility complex protein which plays a role in immune tolerance of the placenta (Tersigni et al., 2020), as well as matrix metallopeptidase 2 (*MMP2*) which is necessary for breaking down the extracellular matrix to enable EVT invasion (Dasilva-Arnold et al., 2015).

Although the differentiated trophoblast subtypes are well characterised in terms of their functions and the specific genes they express, the transcription factor network regulating the balance between CTB self-renewal and differentiation remain to be elucidated.

3.4. ELF5 and the regulation of placentation

Human placentation is regulated by incompletely characterised transcription factor networks that specify the trophoblast lineage and maintain self-renewal in early trophoblast progenitor cells, by expressing key genes such as *GATA3*, *TEAD4*, *TP63*, *TFAP2C* and *MSX2* (Saha et al., 2020, Paul et al., 2017, Kuckenberg er al., 2012, Li et al., 2014, Hornbachner et al., 2021). One of the putative master regulators in this network is E74-like ETS transcription factor 5 (ELF5), for which bisulphite DNA sequencing has shown hypermethylation and repression in embryonic stem cells (ESCs), but hypomethylation and expression in the trophoblast lineage

(Hemberger et al., 2010). ELF5 is absent from the pre-implantation embryo (Blakeley et al., 2015) and likely acts as one of the gatekeepers reinforcing commitment to the trophoblast identity after initial lineage determination. Furthermore, the identification of a compartment of highly proliferative *ELF5*-expressing cells suggests that it might define a population of trophoblast progenitors in the first and early second trimester human placenta (Hemberger et al., 2010). Aside from placentation, ELF5 has also been associated with lineage commitment in mammary gland development, and high expression levels correlate with more aggressive breast cancers (Frend and Watson, 2013, Piggin et al., 2016).

Due to the ethical and logistical obstacles in investigating the early human placenta, most of what is known about the key mechanisms of trophoblast differentiation has resulted from studying murine placentation (Latos et al., 2016). As in humans, this is a haemochorial placentation resulting in direct contact of maternal blood with syncytiotrophoblast as an exchange interface (Fig. 3). The derivation of self-renewing, multipotent mouse trophoblast stem cells (TSCs) over 20 years ago has provided a valuable *in vitro* model for investigating transcriptional regulation (Tanaka et al., 1998). High levels of *Elf5* expression are considered a hallmark of these mouse TSCs and, similar to human *ELF5*, a trophoblast specific *Elf5* hypomethylation pattern has been observed (Ng et al., 2008). Mice with a loss of function mutation in the *Elf5* gene died before E7.5, indicating that this factor is essential during mouse embryogenesis (Zhou et al., 2005, Donnison et al., 2005). On the other hand, *Elf5* overexpression also causes embryonic lethality (Latos et al., 2015), indicating that precise levels are required for the maintenance of a TSC compartment in the placenta. The molecular mechanism behind this has been elucidated, placing Elf5 at the center of a transcription factor hub in which it interacts with Eomes and Tfap2c to promote TSC self-renewal in the presence of high Eomes levels, and differentiation in the presence of low Eomes levels (Latos et al., 2015). Hence, Elf5 has been characterised as both a trophoblast lineage gatekeeper and as a master

regulator of the balance between trophoblast proliferation and differentiation in the mouse.

Despite several similarities between human and murine placentation, the placenta is a very evolutionarily diverse organ. Significant structural (Fig. 3) and molecular differences between the two species make it difficult to extrapolate knowledge (Hemberger et al., 2019). Indeed, a number of transcription factors that are crucial for the maintenance of mouse TSCs including Sox2, Esrrb and Eomes are not expressed in human CTBs (Hemberger et al., 2019). Conversely, MSX2 is a repressor of the ST lineage that is specific to human trophoblast (Hornbachner et al, 2021). These species-specific factors hint at substantially different regulatory networks. Thus, to determine whether ELF5 has a conserved role in humans as a regulator of self-renewal and differentiation, it is important to study models of human placentation.

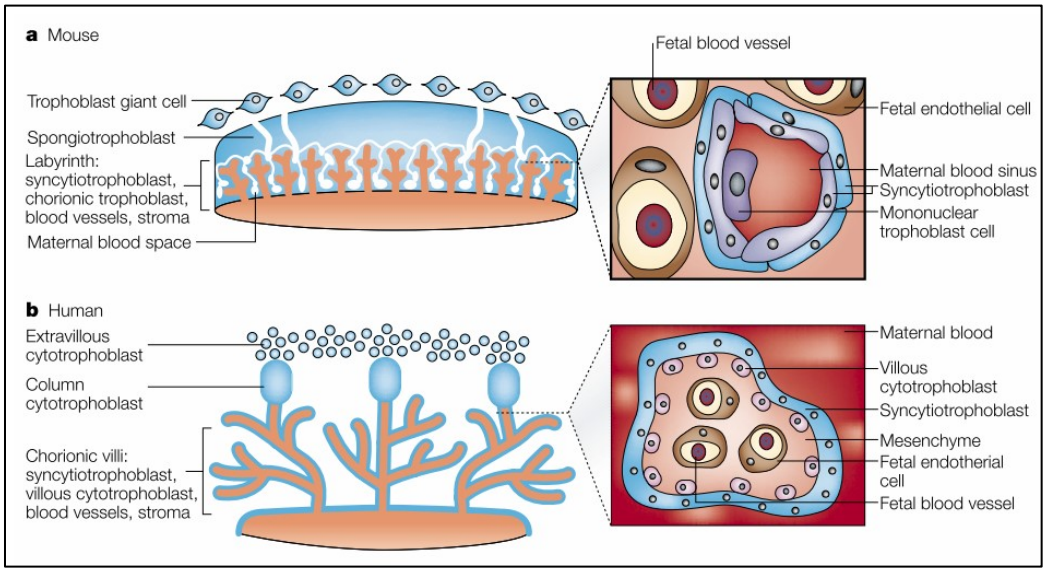

Figure 3. Comparative anatomy of the mouse and human placenta.
In both humans and mice, the villi are covered in syncytiotrophoblasts that lie in direct contact with the maternal blood. *Adapted from Maltepe et al., 2010*.

3.5. Established models of the human placenta

The pathogenesis of most pregnancy disorders develops during the first trimester of pregnancy, when availability of placental tissue is greatly limited. The derivation of human trophoblast cell lines has therefore been an area of focus over the past decade. Primary trophoblasts isolated from first-trimester placentas do not proliferate *in vitro* (Stromberg et al., 1978), and several attempts have been made to overcome this problem.

One of the earlier breakthroughs was the derivation of choriocarcinoma cell lines, which are either naturally occurring in trophoblastic tumors or obtained from the immortalization of primary trophoblast (Speeg et al., 1979, Frank et al., 2000, Heaton et al., 2008). Choriocarcinoma cell lines such as JEG-3, JAR and BeWo have been well characterized for placental research, but although easy to handle and proliferative, these cells do not differentiate fully into trophoblast subtypes (Orendi et al., 2011). Furthermore, several of these cell lines have been found to consist of mixed cell populations containing stromal and mesenchymal cells (Abou-Kheir et al., 2017). An alternative strategy has been the treatment of human embryonic stem cells (ESCs) with bone morphogenic protein 4 (BMP4). In combination with FGF2 inhibition, this results in a downregulation of pluripotency factors NANOG and OCT4, and an upregulation of CDX2, suggesting that it provokes TE lineage differentiation (Amita et al., 2013). Putative CTB-like human trophoblast stem cell lines have been derived, both from BMP-treatment of human induced pluripotent stem cells (Horii et al., 2016) and from single blastomeres of eight-cell embryos (Zdravkovic et al., 2015). However, the trophoblast identity of these cells is questionable as they lack the expression of trophoblast-specific markers, and their HLA status differs from primary cells (Roberts et al., 2014). It was shown more recently that the transdifferentiation of naïve ESCs produces CTB-like cells exhibiting more modest differences to primary trophoblast, in terms of their transcriptomes and methylomes (Cinkornpumin et al., 2020, Dong et al., 2020, Io et al., 2021). Such models may therefore become increasingly useful in the future.

When evaluating these *in vitro* strategies, it is essential to clearly define the trophoblast lineage. Due to the lack of a single marker exclusive to trophoblast, four criteria were proposed to achieve this (Lee et al., 2016). When used in combination, the following criteria would confirm the human first-trimester trophoblast identity of a given cell line. Firstly, the expression of a set of genes highly expressed in trophoblast (such as TFAP2C, GATA3 and KRT7). Secondly, the expression of HLA proteins in a pattern specific to either CTBs, EVTs or STs. Thirdly, high expression levels of the C19MC microRNA complex, and finally, hypomethylation of the *ELF5* promoter (Lee et al., 2016). *ELF5* hypomethylation was indeed shown to be restricted to first-trimester trophoblast (Lee et al., 2016), making it a helpful feature for trophoblast identification while also highlighting the importance of its role.

As the common *in vitro* human trophoblast models that were previously established do not consistently fulfil these criteria (Lee et al., 2016), they are likely unreliable models for studying the early developmental processes that underlie pregnancy disorders.

3.6. hTSCs as a novel model system

The culture conditions used to derive mouse TSCs, i.e. the presence of FGF4, TGF-β and heparin (Tanaka et al., 1998), are not transferable to the derivation of human trophoblast stem cells (hTSCs), which was only achieved much more recently by Okae and colleagues (Okae et al., 2018).

By testing various inhibitors known to enhance *in vitro* proliferation of epithelial stem cells, it was found that activation of wingless/integrated (Wnt) and epidermal growth factor (EGF) signalling, inhibition of the transforming growth factor beta (TGFβ) pathway and inhibition of Rho-associated protein kinase (ROCK) are sufficient for the derivation and long-term expansion of hTSCs (Okae et al., 2018). Therefore, a medium in which EGF, the Wnt activator CHIR99201, the TGFβ inhibitor A83-01

and the ROCK inhibitor Y27632 are combined supports self-renewal and proliferation of hTSCs. hTSCs lines were successfully derived both from CTBs of first-trimester placenta tissue and from blastocysts (Fig. 4).

These cells maintain their ability to differentiate into EVTs and STs after 50 passages, making them highly relevant for studying the regulation of differentiation in detail. Differentiation to EVTs is initiated by the addition of neuregulin-1, knockout serum replacement and Matrigel to the medium, and the removal of EGF and CHIR99201, and is identified by the upregulation of marker genes such as *HLA-G* and *MMP2*. Alternatively, syncytialization into STs is initiated by the addition of forskolin (an adenylyl cyclase activator) and knockout serum replacement to the medium, and the removal of EGF, CHIR99201 and A83-01, and is identified by the upregulation of marker genes such as *CGB* and *SDC1 (*Fig. 4, 5).

Importantly, hTSCs fulfil all four criteria for human first-trimester trophoblast (Lee et al., 2016), which supports their status as the first trophoblast cell line equivalent to self-renewing CTBs of the placental epithelium. Looking at the *ELF5* expression levels, these are slightly lower than in primary CTBs but still significantly higher than in differentiated subtypes (Fig. 5) due to a hypomethylated promoter in hTSCs (Okae et al., 2018). hTSCs display the key capability of proliferation, a maintained ability to differentiate, and a highly homogenous population. Thus, this stem cell line overcomes the limitations of previous trophoblast models.

In addition to this 2D culture system, CTB-derived stem cells can be cultured in a 3D system to form self-organized structures called trophoblast organoids (TB-ORGs) (Haider et al., 2018, Turco et al., 2018). TB-ORGs are derived in similar conditions as 2D hTSCs but the cells are embedded in Matrigel domes. The inner part of TB-ORGs undergoes spontaneous fusion into STs. In contrast, the outer part can be induced to differentiate into EVTs and form cell columns upon removal of Wnt activators (Fig. 6). Hence, TB-ORGs are highly physiologically relevant for studying differentiation, and overall, both 2D and 3D hTSC cultures provide an

excellent model to study the molecular mechanisms driving early human placental development.

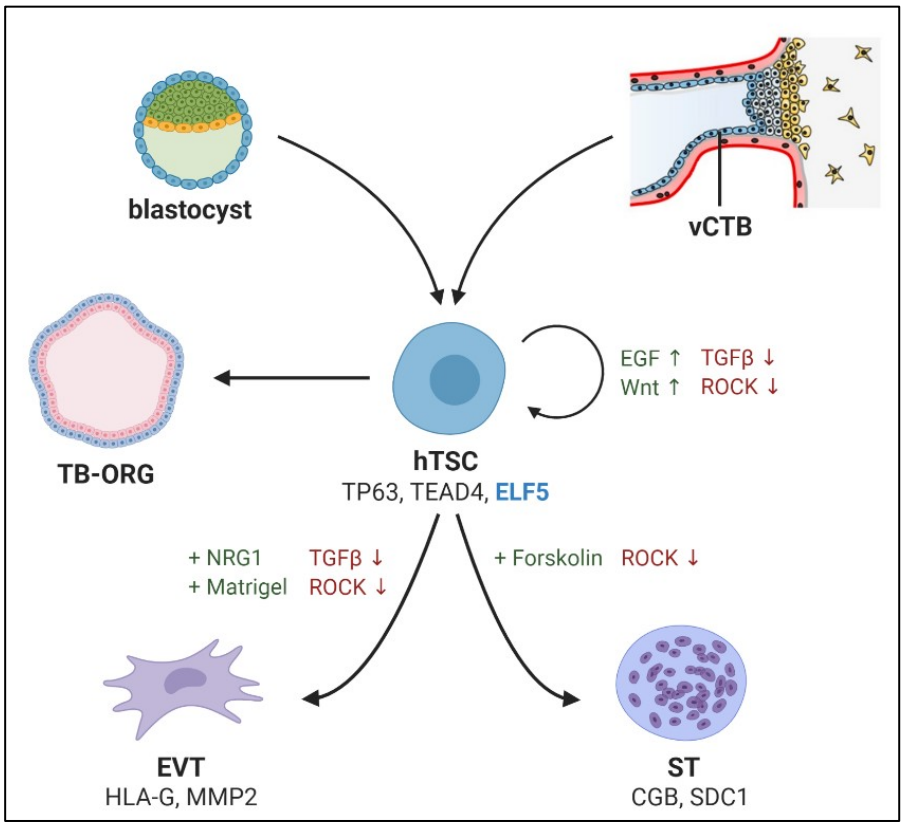

Figure 4. Schematic representation of hTSC culture and *in vitro* differentiation.
hTSCs can be derived from the blastocyst or from villous CTBs of the first trimester placenta and can be cultured either in 2D or in 3D as TB-ORGs. The key marker genes defining the identity of stem cells, EVTs and STs are indicated.

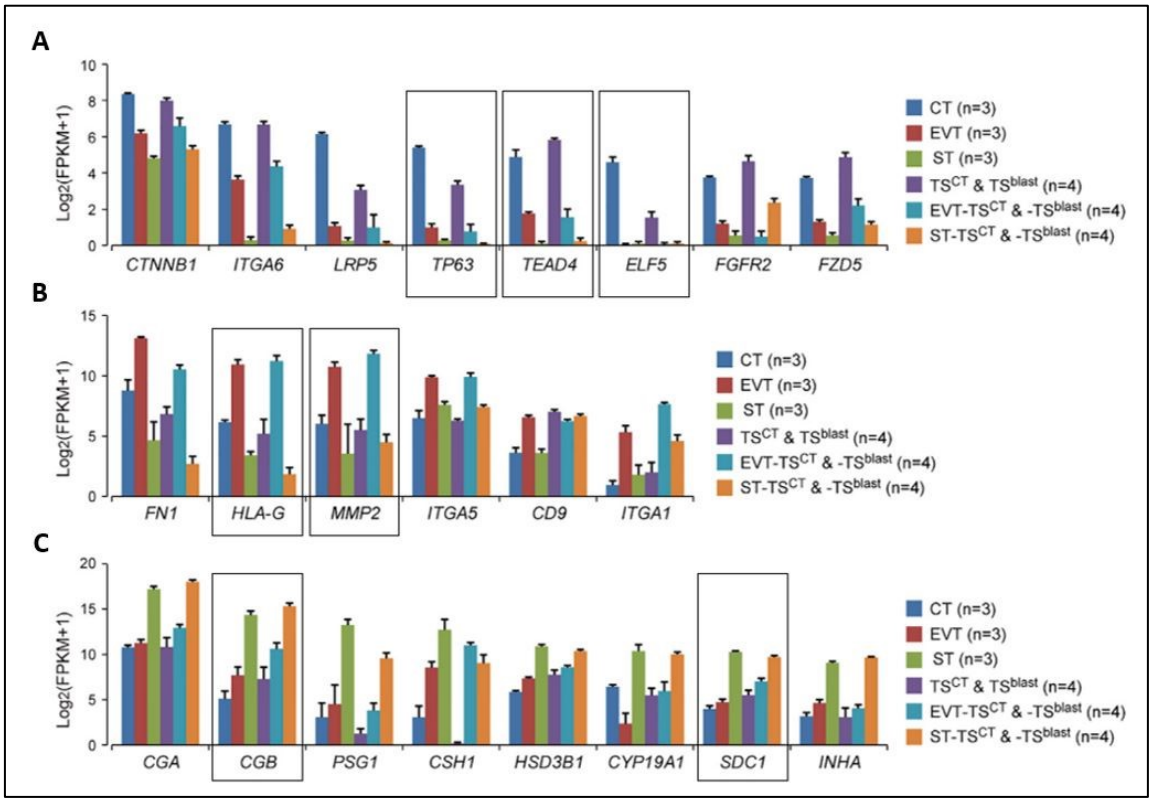

Figure 5. Expression levels of (A) CT, (B) EVT and (C) ST marker genes as measured by RT-qPCR.
The marker genes selected for analysis in this thesis are highlighted, as well as *ELF5*. *Adapted from Okae et al., 2018.*

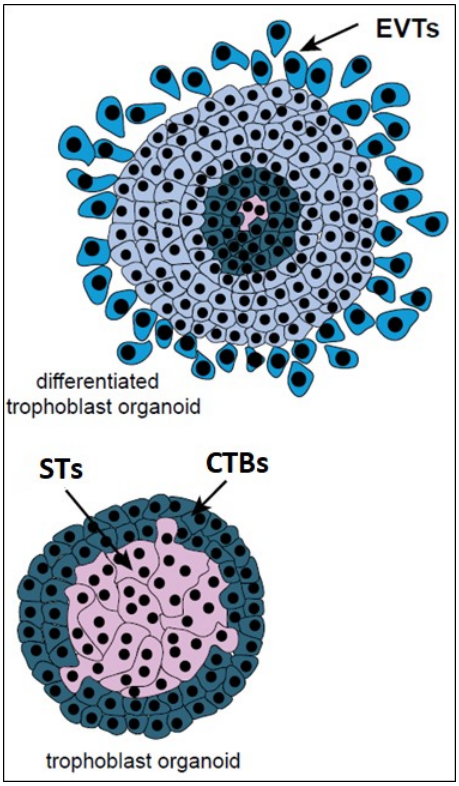

Figure 6. Schematic of differentiated and undifferentiated trophoblast organoids (TB-ORGs).
CTBs spontaneously fuse to form STs and differentiated into EVT outgrowths upon removal of Wnt activators.

3.7. Experimental aims

Trophoblast development occurs in a highly organized manner, both spatially and temporally. Despite this, little is known on the key regulatory factors which control the commitment and differentiation of human trophoblast cells, due to a lack of relevant stem cell models thus far.

The aim of this thesis is to investigate the role of the transcription factor ELF5 in early human placentation by using hTSCs as an *in vitro* model. Functional testing of ELF5 is performed in hTSCs through depletion and overexpression, aiming to elucidate its function in regulating self-renewal and differentiation to STs and EVTs. To enable further functional analysis of this protein, a hTSC line with an ELF5-V5 epitope tag is generated as well as a reporter line with an ELF5-EFP marker.

The data previously published on ELF5 suggests that precise expression levels in early CTBs may reinforce commitment to the trophoblast lineage and that it is likely involved in a transcription factor network regulating their differentiation. The crucial role of Elf5 in the mouse as a molecular switch between self-renewal and differentiation may therefore be conserved in humans, and this thesis makes use of the establishment of hTSCs to test this at the molecular level. Previously, research had been primarily dependent on the availability of placental tissue from different stages of pregnancy, or on model systems that do not adequately represent *in vivo* progenitors. Studying the transcriptional networks at play in hTSCs overcomes these limitations and is expected to provide greater insight into the mechanisms underlying defective human placentation.

4. Materials and Methods

4.1. hTSC maintenance and differentiation

The first trimester cytotrophoblast-derived CT27 hTSC line from Dr Hiroaki Okae (Tohoku University, Japan) was used in all experiments. hTSCs were cultured in DMEM/F12 medium supplemented with 90 μM 2-mercaptoethanol, 0.2% FBS, 1X Antibiotic-Antimycotic, 1% ITS-X supplement, 1.5 μg/ml L-ascorbic acid, 100 ng/ml EGF, 3 μM CHIR99021, 1 μM A83-01 and 5 μM Y27632 (Okae et al., 2018). The cells were cultured at 37°C in 5% CO_2, on plates coated with 10 μg/ml fibronectin at 37°C for one hour. The culture medium was changed every two days and when the cells reached 60%-80% confluency they were split at a ratio of 1:2-1:4. This was done by dissociation with TrypLE for 10-15 minutes at 37°C followed by centrifugation at 1500 rpm for 3 minutes and resuspension in fresh medium. Cells at passages 10-25 were used for analysis.

For differentiation to STs, hTSCs were seeded in a 6-well plate coated with 10 μg/ml fibronectin at a density of 1 x 10^5 cells per well and cultured in ST medium composed of DMEM/F12 supplemented with 90 μM 2-mercaptoethanol, 1X Antibiotic-Antimycotic, 1X ITS-X supplement, 2.5 μM Y27632, 2 μM forskolin, and 4% KnockOut Serum Replacement (KSR) (Okae et al., 2018). The medium was changed after 3 days, and the cells were harvested for analysis after 6 days.

For differentiation to EVTs, hTSCs were seeded in a 6-well plate coated with 20 μg/ml fibronectin at a density of 1 x 10^5 cells per well and cultured in the EVT medium composed of DMEM/F12 supplemented with 90 μM 2-mercaptoethanol, 1X Antibiotic-Antimycotic, 1X ITS-X supplement, 100 ng/ml NRG1, 7.5 μM A83-01, 8 μM Y27632, and 4% KSR (Okae et al., 2018). Shortly after plating the cells, Matrigel was added to each well to a final concentration of 2%. The medium was changed after 3 days, with Matrigel added to a final concentration of 0.5%, and the cells were harvested for analysis after 6 days.

4.2. Culture of TB-ORGs

For the establishment of TB-ORGs, hTSCs at 60-80% confluency were dissociated with TrypLE, centrifuged for 3 minutes at 15000 rpm, and resuspended in DMEM/F12 medium supplemented with 10 mM HEPES, 1X B27, 1X N2, 2 μM glutamine, 100 ng/ml EGF, 3 μM CHIR99021 and 1 μM A83-01. $1x10^4$ cells were resuspended per 40 μl of this medium, and Matrigel was added to this suspension to a final concentration of 60% (60 μl per 40 μl of medium). After mixing by pipetting, 100 μl of this solution was placed in the centre of each well of 24-well plates to form a dome. The plates were incubated 3 minutes at 37°C, then flipped and incubated a further 15 minutes to ensure even distribution of the cells in the solidifying domes. Subsequently, 500 μl of prewarmed organoid medium was added to each well. The medium was changed every 5 days.

4.3. Lipofection

For each reaction, 500 μl Opti-MEM medium was mixed with 15 μl Lipofectamine-3000 (Invitrogen), 5 μl P-3000 (Invitrogen), 8 μg of ELF5-overexpression vector (PB-Avi-hELF5-3xFLAG-IN) or empty vector control, and 3 μg of PBase transposase-expressing vector. The mixture was incubated for 20 minutes at room temperature. In the meantime, a 10 cm dish of confluent hTSCs was dissociated with TrypLE, centrifuged for 3 minutes at 1500 rpm, and resuspended in 1 ml Opti-MEM supplemented with 100 ng/ml EGF, 3 μM CHIR99021, 1 μM A83-01 and 5 μM Y27632. A control reaction without DNA was also performed. The cells for each reaction were plated onto a 3 cm non-adherent dish and the lipofection mixture was added dropwise. After 6 hours of incubation at 37°C, the cell suspension was collected with a pipette, centrifuged for 3 minutes at 1500 rpm, resuspended in 10 ml of hTSC medium and plated on a fibronectin-coated 10 cm dish. The cells were then incubated overnight at 37°C, following which positive clones were selected with

the appropriate antibiotic (500 μg/ml G418 or 0.5 μg/ml puromycin) until all the control cells had died.

4.4. Lentiviral transduction

Lentiviral particles were produced by transfecting HEK293T cells with 1.375 μg psPAX, 1.375 μg pMD2 and 2.5 μg of the shRNA-expressing vector in the lipofection protocol previously described. The HEK293T cells were cultured in DMEM/F12 medium supplemented with 10% FBS, 1X Antibiotic-Antimycotic and 90 μM 2-mercaptoethanol. After transfection of the HEK293T cells and overnight incubation at 37°C, this medium was changed to hTSC base medium (without growth factors), followed by a further 2-day incubation at 37°C. Subsequently, the medium was collected, cell debris was removed by filtration through a 0.45 μm filter, and this viral solution was diluted three-fold in hTSC full medium (to result in the growth factor concentrations listed above). A 10 cm dish of hTSCs at 80% confluency was transduced per shRNA-construct by an overnight incubation at 37°C in this medium, and selection was started two days later with 500 μg/ml G418.

4.5. Preparation of gRNA and Cas9 for knock-in

Custom single-stranded oligonucleotide (ssODN), CRISPR RNA (crRNA) and trans-activating CRISPR RNA (tracrRNA) were designed using the programme Geneious and ordered from Integrated DNA Technologies (See Supplementary Data for sequences). The 67-mer tracrRNA contains the gRNA-scaffold sequence, and the 36-mer crRNA contains a variable gene-specific 20-nucleotide target sequence followed by a 16-nucleotide sequence that base-pairs with the tracrRNA. The ssODN repair template includes the 42-nucleotide V5 tag sequence and a STOP codon flanked by 75-mer homology arms on each side. After resuspension of the lyophilised crRNA and tracrRNA in 20 μl IDTE Buffer, 3.2 μl of each were mixed with 9.9 μl IDTE Buffer on ice and annealed with the following thermocycling steps:

94°C	4 min
93°C	4 min, -0.05°C/sec
80°C	4 min
79°C	1 min, -0.05°C/sec
75°C	4 min
74°C	1 min, -0.05°C/sec
70°C	4 min
69°C	20, -0.05°C/sec
10°C	Hold

Shortly before nucleofection, the RNP was assembled by mixing 16.3 µl of the crRNA/tracrRNA duplex, 1.7 µl of Cas9 (from 4.3 mg/ml stock) and 2 µl of 10X Cleavage Buffer (IDT), and incubating the mixture 5-10 minutes at room temperature.

4.6. Nucleofection

Electroporation was performed using the Neon™ Transfection System (Thermo Fisher) according to the manufacturer's protocol, to deliver the RNP and ssODN into the nucleus for the CRIPSR/Cas9 knock-in. Briefly, $1x10^6$ cells were used in a 100 µl reaction with all of the assembled RNP and 2 µl of the resuspended ssODN. The electroporation protocol used was 2 pulses of 20 ms at 1150 V. Following electroporation, the cells were plated on a 10 cm dish and allowed to recover for 3 days in hTSC medium supplemented with 2 µM M-3814 (a non-homologous end joining inhibitor) before the generation of clones. For the control, a 10 µl control reaction was performed with $1x10^5$ cells and 0.5 µg of pCAG-DsRed vector (Addgene), plated on a 24-well plate. The efficiency of electroporation was

monitored by the expression of dsRed in these cells after 3 days, with an efficiency of >50–70% sufficient for a potentially successful knock-in.

4.7. Immunofluorescence

Placental tissue from the 7th and 10th weeks of gestation was fixed and embedded in paraffin as described (Haider et al., 2016). 3 μm sections were cut using a microtome, mounted on glass slides, and subsequently heated at 70°C to melt the paraffin. Sections were deparaffinized by a 12-minute incubation in Xylol and rehydrated by subsequent 3-minute incubations in 90%, 80% and 70% ethanol. Antigen retrieval was performed in a 2100 Antigen Retriever (Aptum Biologics Ltd) using pH 6.0 Citrate Buffer (Sigma-Aldrich). For immunofluorescence staining of cells, they were grown on fibronectin-coated glass slides and fixed with 4% paraformaldehyde in PBS for 20 min at 4°C.

Cells and sections were permeabilized and blocked for 30 min in 4% donkey serum and 0.1% Triton X-100 in PBS, and incubated with primary antibodies (listed in table S1) overnight at 4°C. The slides were then washed three times with PBS and incubated with Alexa Fluor secondary antibodies (Thermo Fischer, listed in table S1) for one hour in the dark. Nuclei were stained with 1 μg/ml DAPI and the slides were mounted with Fluoromount-G™ Mounting Medium (Thermo Fischer). Tissue sections and cells were analysed by epifluorescence microscopy (Zeiss Imager A2, ZEN 2012) and digitally photographed.

4.8. Nuclear protein extraction

A high salt nuclear extract was prepared from two wells of a 6-well plate at 80% confluency. The cell pellet was resuspended in 500 μl Hypotonic Buffer (10 mM

HEPES, 1.5 mM $MgCl_2$, 10 mM KCl, 1X Protein Inhibitor Cocktail (Sigma-Aldrich), 0.5 mM DTT, 1 mM PMSF) and incubated on ice for 15 minutes. 15.8 µl 10% NP-40 was added and the mixture was vortexed for 30 seconds and centrifuged at 10 000 rpm for 1 minute at 4°C. The supernatant was discarded, 20 µl Cell Extraction Buffer (20 mM HEPES, 12.5% Glycerol, 1.5 mM $MgCl_2$, 20 mM KCl, 0.2 mM EDTA (pH8), 400 mM NaCl, 1X Protein Inhibitor Cocktail (Sigma-Aldrich), 0.5 mM DTT, 1 mM PMSF) was added and the mixture was placed on a shaker for 1 hour at 4°C. A second centrifugation at 14 000 rpm for 10 minutes at 4°C was performed, following which the supernatant was transferred to a fresh, pre-cooled tube and the protein concentration was measured in a Bradford assay.

4.9. SDS PAGE and Western blot

The protein samples were incubated for 5 minutes at 95°C in 2X Laemmli Buffer (50 mM Tris-HCl pH 6.8, 2% SDS, 10% glycerol, 1% β-mercaptoethanol, 12.5 mM EDTA, 0.02% bromophenole blue) before loading onto a 10% SDS gel with the following composition:

Reagent	**Stacking Gel (2.5mL)**	**Resolution Gel (10mL)**
Acrylamide/bis, 305	410µl	3.4mL
Tris pH 8.8, 1M	/	3,75mL
Tris pH 6.8, 1M	310µl	/
SDS, 20%	12.5µl	100µl
TEMED	2.5µl	8µl
APS, 10%	25µl	200µl

Proteins were then separated at 14 mA through the stacking gel and 28 mA through the resolution gel in 1X SDS Running Buffer (25 mM Tris, 192 mM glycine, 0.1% SDS). A transfer was performed from the SDS gel to a methanol activated nitrocellulose membrane at 250 mA for 2 hours in precooled transfer buffer (10% methanol, 20% Tris-Glycine). The membrane was then washed with 0.1% Tween-20 in PBS, blocked for 30 minutes with 5% milk powder and 0.1% Triton X-100 in PBS, and incubated with the primary antibody overnight at 4°C. On the next day, the membrane was washed 5 times for 10 minutes with 0.1% Triton X-100 in PBS before incubation with the secondary antibody for 1 hour at room temperature. The membrane was washed 4 times for 10 minutes with 0.1% Triton X-100 in PBS, developed with Clarity Max™ Western ECL Blotting Substrates (Bio Rad) and visualized with the FusionFX6 imaging system (Vilber Lourmat).

4.10. RNA purification and RT-qPCR

Total RNA was prepared using the innuPREP RNA Mini Kit (Analytik Jena). The cells were lysed with the lysis solution provided, transferred to a microcentrifuge column, and centrifuged at 11000 rpm for 2 minutes. An equal amount of 70% ethanol was added to the filtrate before it was loaded into a new column and centrifuged at 11000 rpm for 2 minutes. The column was washed twice with the washing solution provided by centrifugation at 11000 rpm for 1 minute. The RNA was eluted from the column with 20µl RNase-free water by centrifugation at 11000 rpm for 1 minute.

After extraction from the lysed cells, 2µg of the RNA was treated with 1.5µl DNase I (Thermo Fischer) for 15 minutes at 37°C. The DNase was inactivated by the addition of 1.5µl EDTA and incubation for 10 minutes at 65°C.

cDNA was synthesized from total DNA-free RNA by reverse transcription. First, 0.2µg of random primers (Thermo Fischer) was added to the RNA followed by incubation for 5 minutes at 65°C. The following reagents were then added to this

mixture: 0.5µl of RNase inhibitor (RiboLock R1 40U/µl, Thermo Fisher Scientific), 2µl of dNTPs (10mM, Thermo Fisher), 1µl of DNA Polymerase (Revert Aid H Minus 200U/µl, Thermo Fisher) and 4µl of buffer (5x Reverse Transcription buffer, Thermo Fisher). The reaction was incubated for 10 minutes at 25°C followed by 60 minutes at 42°C and 10 minutes at 70°C.

The cDNA obtained was diluted 1:31 and real-time PCR was performed using GoTaq Polymerase Master Mix (Promega) on a CFX Connect Real Time detection system (Biorad). The amount of target mRNA was determined using the ΔΔCt method with *PBGD* as the internal control for normalisation.

5. Results

5.1. ELF5 expression *in vivo*

In order to identify the localisation of ELF5 expression in early placental tissue, immunofluorescence (IF) staining was performed on paraffin-embedded human placental tissue from weeks 7 and 10 of development. This revealed that nuclear ELF5 is present in the CTB layer of chorionic villi as well as in some stromal cells inside the villi but is absent from the outer ST layer (Fig. 7). The ELF5 expression levels in CTBs appears to be rather heterogenous, with some cells displaying much higher signals than others. It can also be observed that ELF5 signal intensity is slightly lower at 10 weeks than at 7 weeks, suggesting a decrease in expression levels during development. *In situ* hybridisation experiments have previously shown that ELF5 expression is higher at 5 weeks than at 15 weeks (Soncin et al., 2018), further suggesting a downregulation of ELF5 during development.

Another staining was performed on serial sections of a 6-week placental sample using the EVT marker HLA-G to identify cell columns, in order to determine the expression pattern of ELF5 during cell column formation (Fig. 8). This staining shows that HLA-G is only expressed in terminally differentiated EVTs at the tip of the cell column, and that ELF5 is not expressed in any part of the cell column, as it is downregulated at the onset of EVT progenitor specification. Although a high background signal is observed for ELF5 (Fig. 8A), this is not specifically nuclear and cannot be interpreted as the presence of the protein.

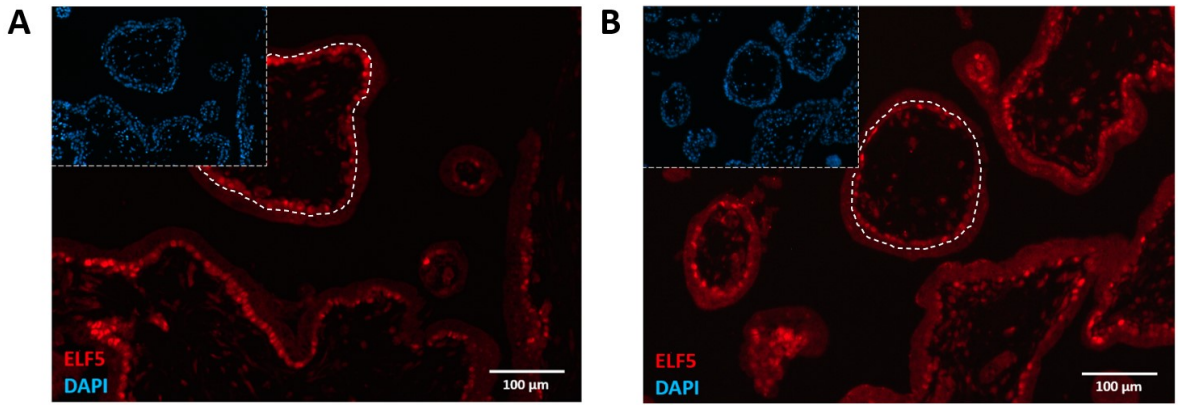

Figure 7. Immunofluorescence staining of first-trimester placental sections for ELF5.
(A) Chorionic villi cross sections of a 7-week placenta sample. (B) Chorionic villi cross sections of a 10-week placenta sample. Nuclear ELF5 is detected in the villous CTB layer of the villi as well as in villous stromal cells but is absent from the STB layer of the villi. Dashed lines demarcate the CTB layer from the ST layer. DAPI is used as a nuclear marker.

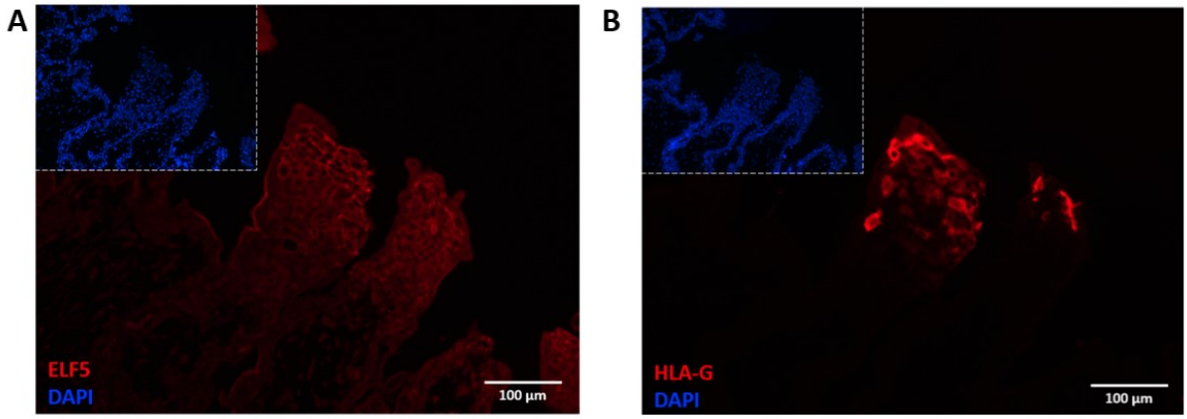

Figure 8. Immunofluorescence staining of 6-week placental cell columns for ELF5 and HLA-G.
Two serial placental sections were stained for (A) ELF5 and (B) HLA-G respectively, and DAPI was used as a nuclear marker. Two cell columns are visible with HLA-G-positive EVTs at their distal ends, and no nuclear ELF5 is detected within the cell columns. DAPI is used as a nuclear marker.

RNA sequencing (RNA-seq) data is also a valuable resource for evaluating *in vivo* expression patterns. Liu et al. recently performed single-cell RNA-seq on sorted human placental cells from the first and second trimester (Liu et al., 2018), the resulting data of which I downloaded to analyse the level and homogeneity of *ELF5* expression. The authors sorted the cells into five distinct populations based on surface markers (CTBs, STs, 8-week EVTs, 24-week EVTs and stromal cells) and

sequenced 1567 transcriptomes in total. For each cell, I compared the *ELF5* expression levels to two common CTB markers, *TP63* and *TEAD4* (Fig. 8). This analysis revealed that while *ELF5* is not expressed in EVTs and STs, it is not completely specific to CTBs as many stromal cells display high RPKM values for *ELF5*. Furthermore, the expression levels in CTBs are highly heterogenous, with many CTBs displaying a RPKM value of 0. Upon linear regression analysis, the positive correlation is lower than expected between *ELF5* and CTB markers (R^2 values 0.0279 and 0.0409 for *TEAD4* and *TP63* respectively), once again indicating high variability in RPKM values between cells (Fig. 9). This could either be explained by a lack of specificity of CTB isolation for this RNA-seq experiment or by CTBs being an intrinsically heterogenous population in terms of their transcriptomes.

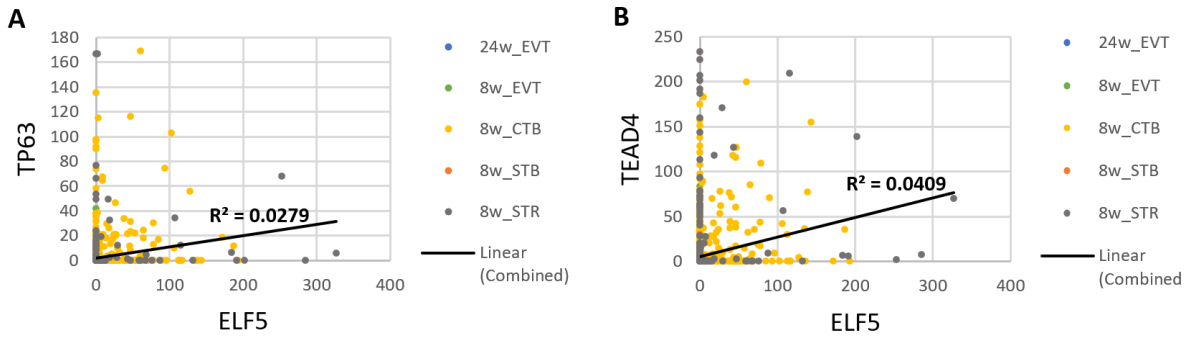

Figure 9. Correlation between ELF5 and self-renewal marker expression from single-cell RNA-seq data. (A) Correlation between ELF5 and TP63 RPKM values. (B) Correlation between ELF5 and TEAD4 RPKM. The sorted placental cell types analysed are CTBs, STs (STB), EVTs and stromal cell (STR) from the 8-week placenta, and EVTs from the 24-week decidua. Low positive correlations are observed, with an R^2 value of 0.0279 between ELF5 and TP63 and an R^2 value of 0.0279 between ELF5 and TEAD4.

5.2. ELF5 expression *in vitro*

The *ELF5* gene has four splice variants in the National Center for Biotechnology Information RefSeq database, predicted to produce four unique proteins (Fig. 10). Isoforms 2 and 3 both have orthologous start sites to mouse *Elf5*, while isoforms 1 and 4 harbour a different transcription start site (Hemberger et al., 2010). Isoforms 3 and 4 are shorter transcripts produced by splicing of exons 4 and 5 respectively,

so they lack the Pointed (PNT) domain but retain the E26 Transforming Sequence (ETS) domain (Piggin et al., 2016). To identify which splice variants is expressed in hTSCs, an isoform-specific RT-qPCR was run on hTSC total mRNA with primer sets that distinguish isoforms 2 and 3 from isoforms 1 and 4 (Fig. 10). The results showed that either isoform 2, isoform 3, or both, are present (Fig. 11A). Since it was not possible to design qPCR primers that distinguish between these two isoforms, a PCR was run with primers that produce amplicon sizes specific to isoforms 2 and 3, and the product was visualized on an agarose gel. The resulting bands indicate that isoform 2 is the relevant *ELF5* splice variant in hTSCs (Fig. 11B).

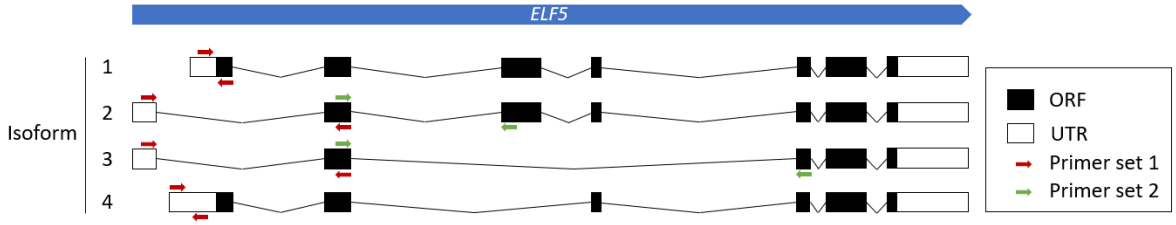

Figure 10. Schematic representation of the four splice variants of the *ELF5* gene.
The coding sequence is shown in blue, and the approximate positions of the open reading frame (ORF) and untranslated region (UTR) parts of the exons are shown in black and white, respectively. The PCR primers used to generate isoform-specific amplicons are shown in red and green.

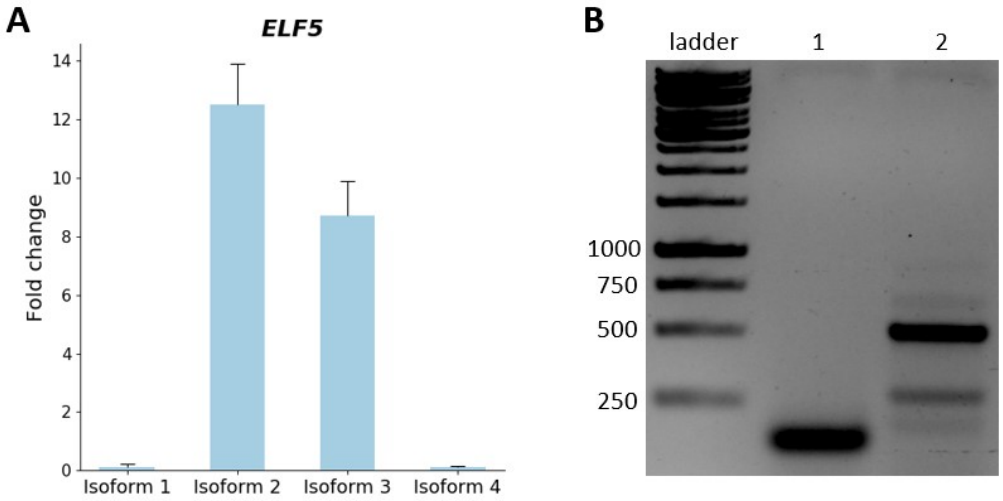

Figure 11. Identification of the relevant ELF5 isoform in hTSCs.
(A) RT-qPCR run with primer set 1, showing that either isoform 2 or 3 is expressed. Expression levels are relative to the average level across all four isoforms. Error bars show standard deviation for 3 technical replicates. (B) PCR run with primer set 2, in which reaction 1 is expected to produce a 141 bp band from isoform and reaction 2 is expected to produce a 122 bp band from isoform 3. The band sizes observed are 141 bp and 500 bp respectively, showing that only isoform 2 is present.

Next, we investigated the effect of hTSC differentiation on *ELF5* expression levels by RT-qPCR. The directed differentiation protocol defined by Okae and colleagues was followed to obtain terminally differentiated EVTs and STs after 6 days, with distinctly elongated and multinucleated morphologies respectively (Fig. 12). RT-qPCR results confirmed these cell identities with the downregulation of self-renewal markers *TP63* and *TEAD4*, the upregulation of EVT markers *HLA-G* and *MMP2* in EVTs and the upregulation of ST markers *CGB* and *SDC1* in STs (Fig. 13B-D). Looking at *ELF5* expression levels, there is a significant downregulation in both differentiated subtypes compared to self-renewal conditions (Fig. 13A), which corroborates the RT-qPCR analysis previously performed by Okae and colleagues (Okae et al., 2018).

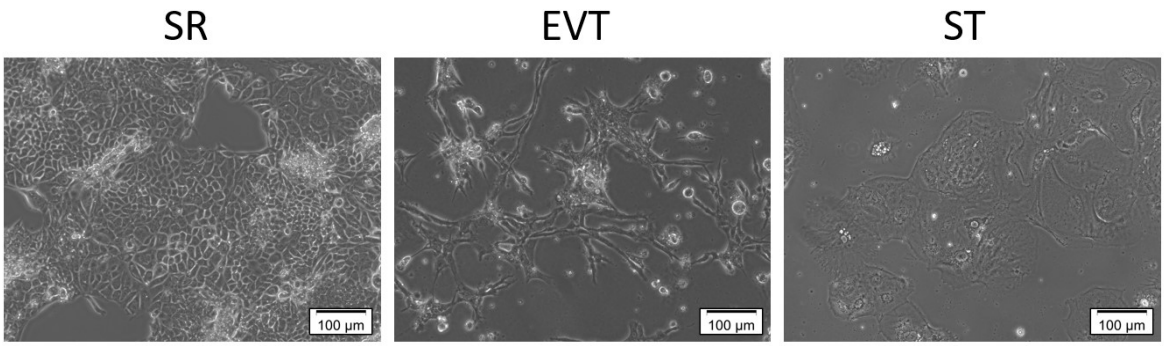

Figure 12. Brightfield microscopy images of wildtype hTSCs under self-renewal (SR) and upon directed differentiation to EVTs and STs.
Self-renewing cells exhibit a cobblestone epithelial morphology, while EVTs exhibit an elongated mesenchymal morphology, and STs form a flat multinucleated layer.

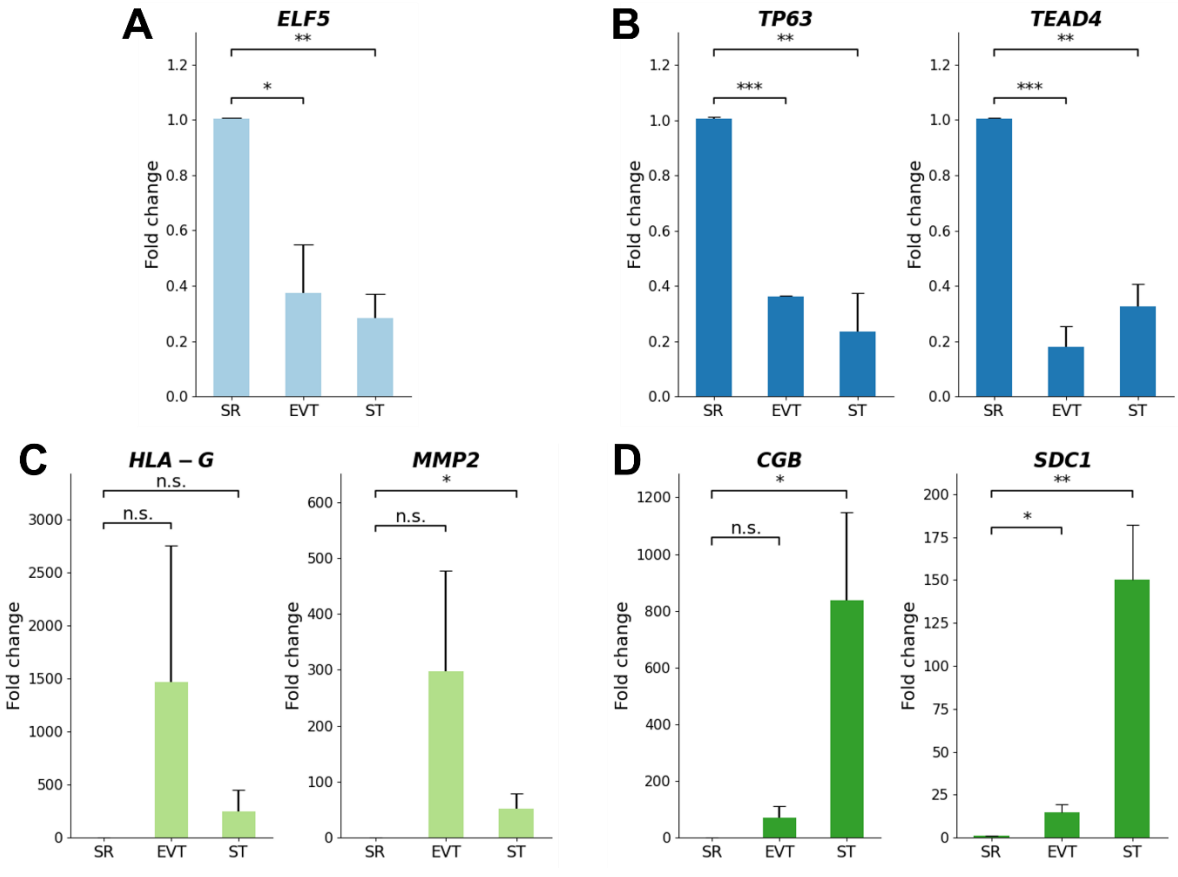

Figure 13. RT-qPCR analysis upon directed differentiation of wildtype hTSCs to EVTs and STs.
(A) *ELF5* is downregulated. (B) Self-renewal markers *TP63* and *TEAD4* are downregulated. (C) EVT markers *HLA-G* and *MMP2* are upregulated. (D) ST markers *CGB* and *SDC1* are upregulated. Error bars show S.E.M. for 3 biological replicates, with 3 technical replicates each. *p<0.1, **p<0.01, ***p<0.001

The process of differentiation from hTSCs to EVTs has very low reproducibility, as most attempts produced cells with neither typical EVT morphology nor a consistent downregulation of self-renewal markers and upregulation of EVT markers. The variability in EVT marker expression is indicated by the large error bars obtained from this wildtype differentiation experiment (Fig. 12C). This is likely due to the fact that EVTs are a highly heterogenous population (Cierna et al., 2016) with variable transcriptomes, and are also highly invasive, which makes them difficult to consistently obtain *in vitro*. Thus, the rest of the results described will focus on differentiation to STs only, as this produced more consistent outcomes.

5.3. Generation of an ELF5 knock-down line and differentiation

To investigate the role of ELF5, the first strategy we selected was its depletion using a short-hairpin RNA knock-down (shRNA KD). hTSCs were transduced with the pLKO.1 system lentiviral vector carrying Neomycin resistance for selection, and three different shRNA sequences targeting the *ELF5* gene were tested (Fig. 14). An shRNA sequence targeting the *GFP* gene was used as a control for the effects of the transduction protocol. The efficiency of each shRNA sequence in depleting *ELF5* mRNA levels compared to the GFP-targeting shRNA was monitored by RT-qPCR (Fig. 16A). While all three sequences produced successful KDs, shRNA-2 was found to be the most efficient with an almost 80% reduction in ELF5 levels, so this cell line was used in all subsequent experiments.

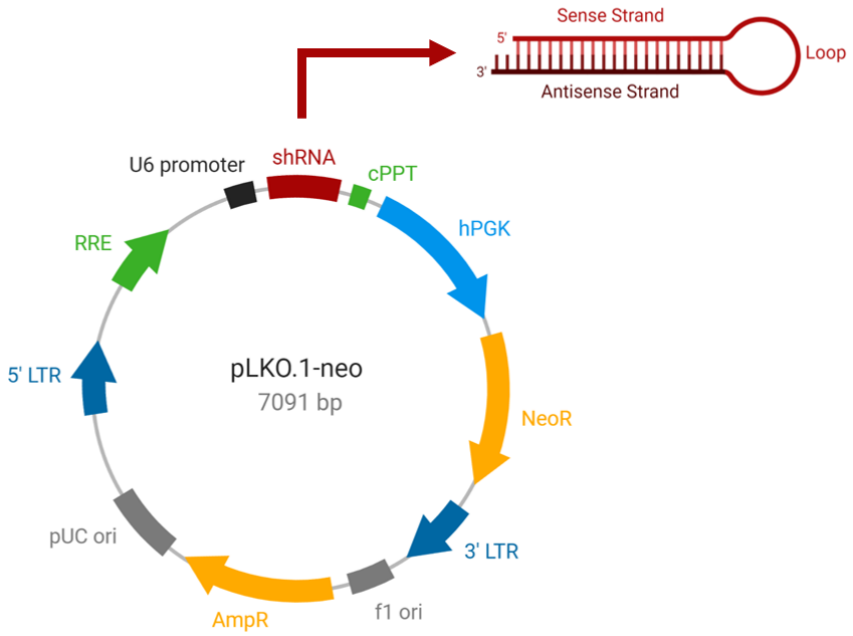

Figure 14. pLKO.1-Neo vector used to generate the ELF5 KD line.
The hairpin structure of the transcribed shRNA construct is depicted schematically. cPPT, central polypurine tract; hPGK, human phosphoglycerate kinase promoter; NeoR, neomycin resistance gene; LTR, long terminal repeat; f1 ori, f1 bacterial origin of replication; AmpR, ampicillin resistance gene; pUC ori, pUC bacterial origin of replication; RRE, rev response element; U6, human U6 promoter.

The ELF5 KD line could be maintained under hTSC self-renewal conditions long-term and without any apparent changes to cell morphology (Fig. 15). RT-qPCR analysis showed no significant reduction in self-renewal markers compared to the control (Fig. 16C). To determine whether ELF5 depletion has any effect on hTSC differentiation potential, a directed differentiation to STs was performed on both the control line and the ELF5 KD line. The changes in cell morphology observed upon differentiation were comparable between the control and ELF5 KD (Fig. 15). Confirming this observation, RT-qPCR analysis showed that the changes in marker gene expression levels correspond to a successful ST differentiation for both lines (Fig. 16D). Thus, this KD experiment showed that hTSCs are not sensitive to depleted ELF5 levels, as they do not lose their proliferative capacities or ability to efficiently differentiate to STs.

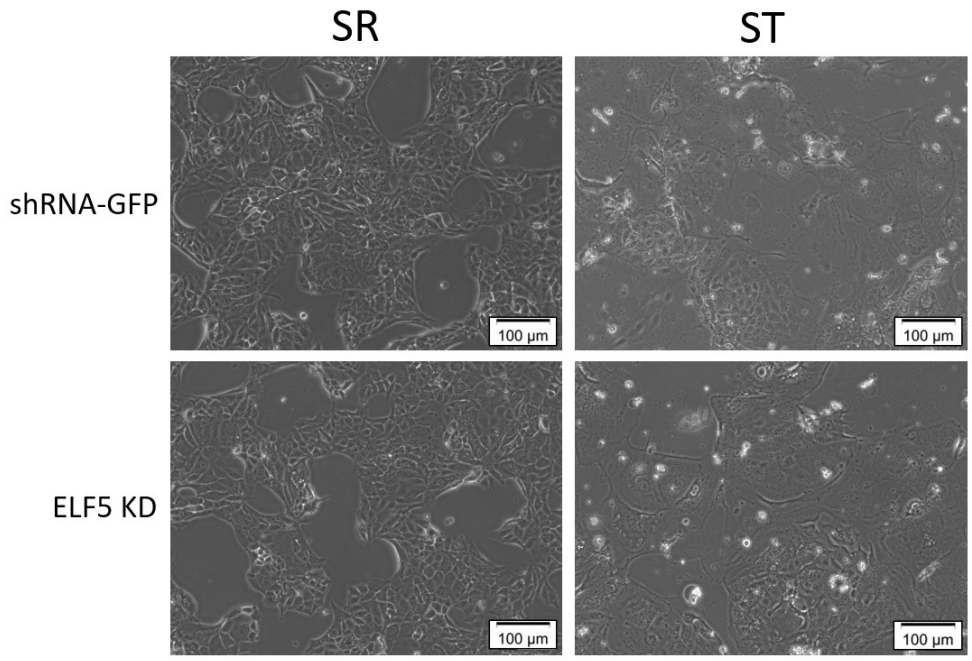

Figure 15. Brightfield microscopy images of the control shRNA-GFP cell line and ELF5 KD cell line under SR and upon differentiation to STs after 6 days.
Cell morphologies are identical between the two cell lines in both states, indicating a null or minimal effect of the ELF5 KD.

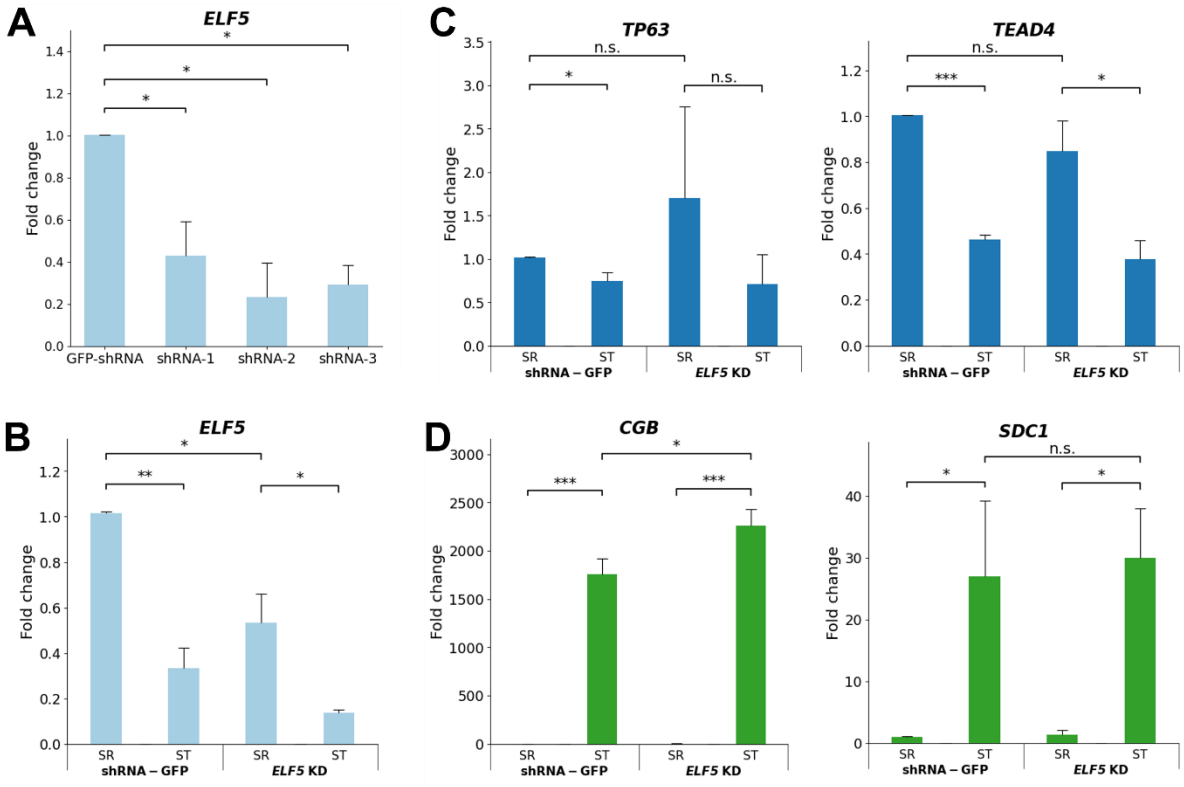

Legend on next page.

Figure 16. RT-qPCR analysis of the ELF5 KD cell line under SR and upon differentiation to ST.
(A) *ELF5* mRNA levels are depleted by the three shRNA constructs tested, relative to the GFP-shRNA control. (B) *ELF5* levels decrease upon differentiation both for the control line and ELF5 KD line. (C) SR markers *TP63* and *TEAD4* are upregulated upon differentiation both for the control line and the ELF5 KD line. (D) ST markers *CGB* and *SDC1* are upregulated upon differentiation both for the control line and the ELF5 KD line. Error bars show S.E.M. for 3 biological replicates, with 3 technical replicates each. *p<0.1, **p<0.01, ***p<0.001

5.4. Generation of an ELF5 constitutive overexpression line and differentiation

In order to further test whether precise ELF5 levels are important for hTSC maintenance and differentiation, constitutive overexpression of ELF5 was generated in a hTSC line (ELF5 cOX). This was achieved by cloning the coding sequence (CDS) of ELF5 isoform 2 into a PiggyBac expression vector, which drives high levels of expression in mammalian cells under control of the CAG promoter (Fig. 17). The ectopic protein is fused with a N-terminal Avi peptide tag and a C-terminal triple FLAG (3xFLAG) tag for antibody detection and biochemical analysis.

hTSCs were co-transfected with this vector and a PBase transposase-expressing vector by lipofection, and selection with neomycin was used to generate a stable ELF5 cOX line. As a control, a second cell line was generated by the same method with an empty vector lacking the ELF5 CDS. PB transposase integrates around 15 copies of exogenous DNA at random locations in the genome, by recognizing the inverted terminal repeats (ITRs) flanking the transgene cassette and inserting them at TTAA sites, which averages out positional effects on expression.

Overexpression of 3xFLAG-tagged ELF5 was validated both on the mRNA levels by RT-qPCR, using 3xFLAG-specific primers (Fig. 20A) and on the protein level by Western blot, using an anti-FLAG antibody (Fig. 18). This confirmed that ectopic ELF5 is present only in the ELF5 cOX line and is expressed at high levels.

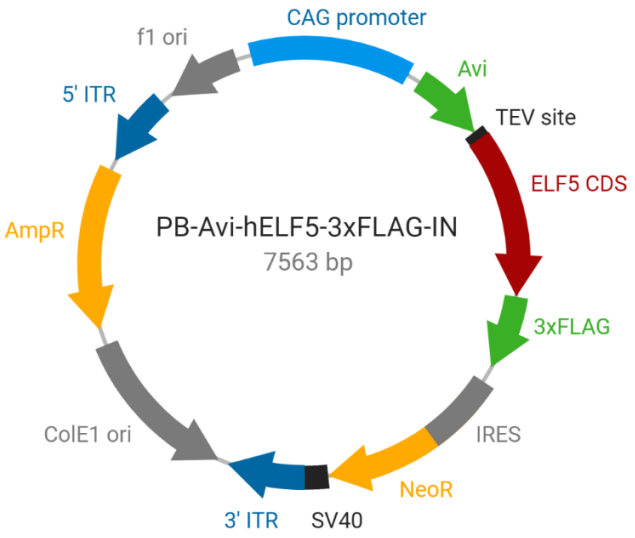

Figure 17. PiggyBac plasmid used to generate the ELF5 cOX line.
CAG, CMV enhancer, chicken beta-actin promoter and rabbit beta-globin splice acceptor site; Avi, Avi peptide tag for biotin labelling; TEV site, tobacco etch virus protease cleavage site; 3xFLAG, triple FLAG peptide tag for antibody detection; IRES, internal ribosomal entry site; NeoR, neomycin resistance gene; SV40, simian virus 40 promoter; ITR, inverted terminal repeat; ColE1 ori, ColE1 bacterial origin of replication; AmpR, ampicillin resistance gene; f1 ori, f1 bacterial origin of replication.

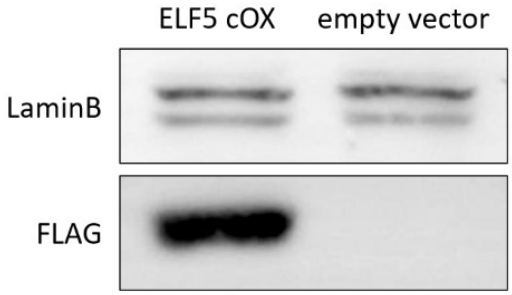

Figure 18. Western blot confirming presence of 3xFLAG-tagged ELF5 in the ELF5 cOX line.
Nuclear protein extract from both cell lines was probed with anti-FLAG antibody, and with anti-LaminB antibody as a loading control.

Interestingly, the established ELF5 cOX line does not exhibit any morphological differences or reduced proliferation compared to the control, and successful differentiation to STs could also be induced in these cells (Fig. 19). Upon differentiation, RT-qPCR analysis using primers that target both endogenous and exogenous ELF5 showed that overexpression levels are significantly higher in STs than in SR (Fig. 20A). This suggests that the transgene is upregulated in STs, and

that for unknown reasons the constitutive CAG promoter drives more stable expression in the differentiated state than in the self-renewal state. Furthermore, upon constitutive overexpression, endogenous ELF5 levels in SR cells drop as compensation (Fig. 20B), possibly indicating a feedback loop in which hTSCs attempt to drive levels back to normal. RT-qPCR also partly confirmed a successful differentiation of ELF5-overexpressing hTSCs to STs with an upregulation of ST markers. However, self-renewal markers are not significantly downregulated (Fig. 20C), and ST markers are not as highly upregulated as in the control (Fig. 20D).

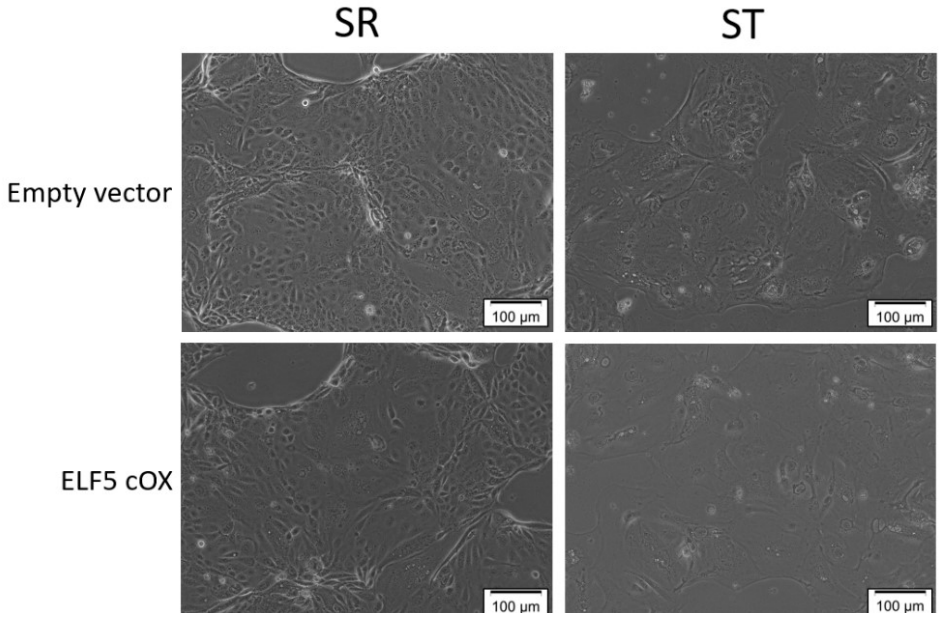

Figure 19. Brightfield microscopy images of the empty vector control line and ELF5 cOX line under SR and upon differentiation to STs after 6 days.
Cell morphologies are identical between the two cell lines in both states, indicating a null or minimal effect of the ELF5 cOX.

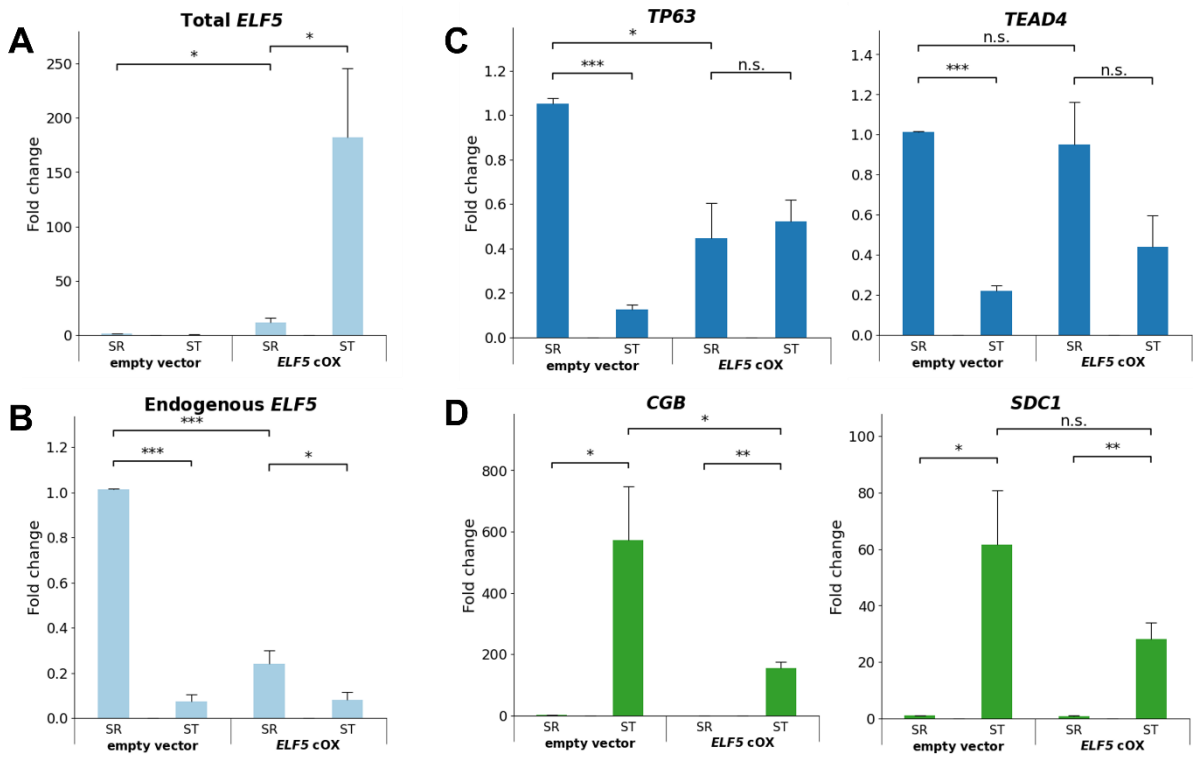

Figure 20. RT-qPCR analysis of the ELF5 cOX line under SR and upon differentiation to ST.
(A) Total *ELF5* levels, including both endogenous and exogenous mRNA, are upregulated in the ELF5 cOX line compared to the empty vector control. (B) Endogenous *ELF5* levels decrease upon overexpression as compensation and decrease upon differentiation both in the control and ELF5 cOX line. (C) *TP63* is downregulated in undifferentiated ELF5 cOX cells. Both *TEAD4* and *TP63* are not significantly downregulated upon differentiation of ELF5 cOX cells. (D) *CGB* and *SDC1* are upregulated upon differentiation both for the control line and the ELF5 cOX line, although the fold change is smaller in ELF5 cOX. Error bars show S.E.M. for 3 biological replicates, with 3 technical replicates each. *p<0.1, **p<0.01, ***p<0.001

5.5. Generation of an ELF5 inducible overexpression line and differentiation

Inducible systems allow for more controllable, time-specific, and efficient overexpression than constitutive systems, so a doxycycline-induced ELF5 overexpression hTSC line (ELF5 iOX) was generated to further investigate the effects of elevated ELF5 levels on self-renewal and differentiation. This was achieved by using the Gateway technology to clone the ELF5 coding sequence under the control of the doxycycline-inducible promoter pTRE-tight. Under the control of this promoter, transcription is activated by the addition of doxycycline (dox) in a so-

called Tet-On system. This involves dox binding reverse tetracycline-controlled transactivator (rtTA), allowing it to bind the Tet response element (TRE), which initiates transcription (Gossen et al., 1995). As was done for the ELF5 cOX line, the ectopic protein was fused to a C-terminal 3xFLAG tag (Fig. 21). The resulting vector was co-transfected with a PBase-expressing vector into hTSCs by lipofection, a stable line was obtained by neomycin selection, and this was repeated with an empty vector lacking the ELF5 CDS to generate a control cell line. This control line was included in the following experiments, however in the displayed results the ELF5 iOX line in the absence of dox is shown as an equivalent control.

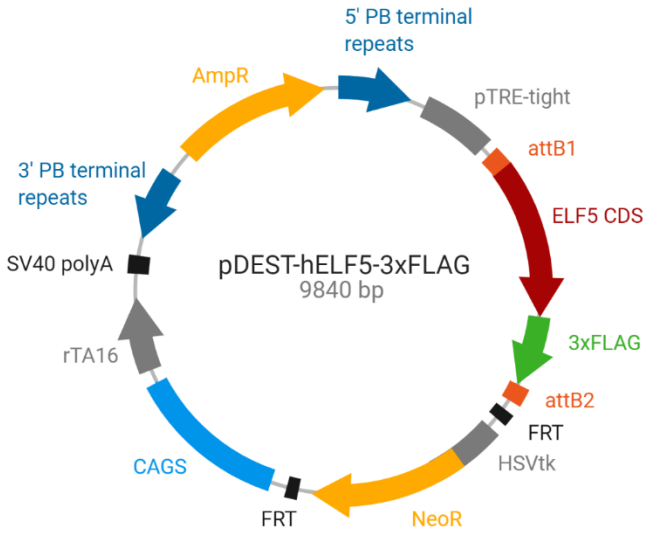

Figure 21. PiggyBac Gateway expression plasmid used to generate the ELF5 iOX line.
pTRE-tight, tet-responsive element promoter; attB1/2, Gateway-specific recombination sites; FRT, Flp/FRT recombination site; HSVtk, Human Thymidine Kinase Gene Promoter; NeoR, neomycin resistance gene; CAGS, CMV enhancer, chicken beta-actin promoter and rabbit beta-globin splice acceptor site; rTA16, reverse tetracycline-controlled transactivator 16; SV40 polyA, Simian virus 40 PolyA terminator sequence; AmpR, ampicillin resistance gene.

Induced expression of 3xFLAG-tagged ectopic ELF5 by dox treatment was validated by immunofluorescence detection with an anti-FLAG antibody (Fig. 22A, B). This staining shows a heterogenous but high expression of ectopic ELF5 in the presence of dox and indicates that this system is tightly controlled as no ectopic

ELF5 was detected in the absence of dox. An anti-ELF5 antibody was used to detect both endogenous and exogenous ELF5, however this revealed very low levels in the absence of dox, as a nuclear signal was only detected in the ELF5 iOX line (Fig. 22A, B). This could be explained by either a low specificity of the antibody used, leading to a high background signal, or by endogenous ELF5 levels that are too low to be detected at the protein level in hTSCs.

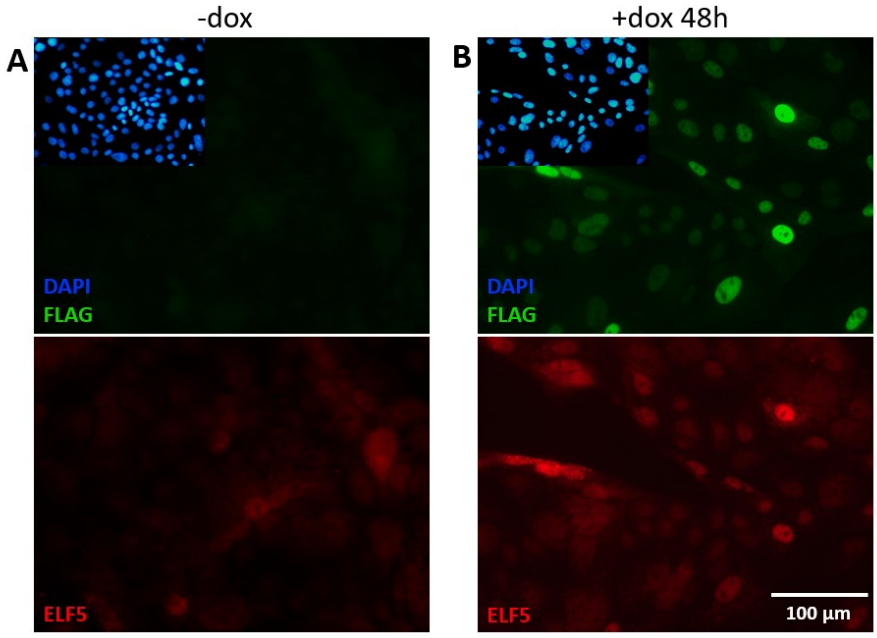

Figure 22. Immunofluorescence staining showing the induction of 3xFLAG-tagged ELF5 expression by 48h doxycycline (dox) treatment.
Nuclear 3xFLAG is not detected in the absence of dox (A) and is detected in the presence of dox (B), indicating a tight control of expression. The ELF5 antibody could only be detected upon overexpression, indicating low endogenous levels in hTSCs. DAPI is used as a nuclear marker.

Cell morphology and proliferation of the self-renewing ELF5 iOX line was initially evaluated by frequent brightfield microscopy observations during 48h and 6 days of dox treatment, and the images taken showed no significant consequences over time (Fig. 23). The 6-day differentiation protocol was once again followed to assess the potential of ELF5 iOX cells to differentiate to STs upon induction by dox. Once again, no significant differences were observed between STs derived in the absence and presence of dox (Fig. 24).

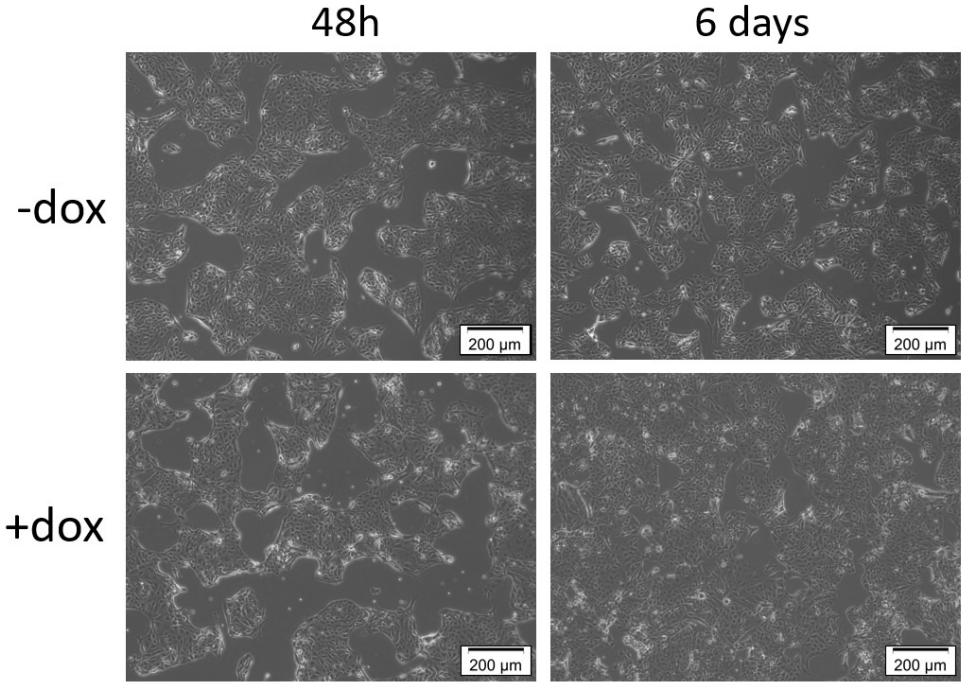

Figure 23. Brightfield microscopy images of the ELF5 iOX line with and without doxycycline (dox) 48 hours and 6 days after plating.
Cell morphology and proliferation are not visibly affected by the induction of ELF5 expression.

RT-qPCR analysis confirmed that ELF5 iOX cells still maintain differentiation capabilities under dox treatment, with a clear downregulation of *TEAD4* and upregulation of *CGB* and *SDC1* mRNA levels (Fig. 25C, D). In order to further test the robustness and efficiency of ST differentiation in induced ELF5 iOX cells, ST markers CGB and ENDOU were measured on the protein level by immunofluorescence (Fig. 26). Indeed, these two cytoplasmic proteins are not detected in the SR state and become highly expressed in the ST state both in the absence and presence of dox. Detection of ectopic ELF5 by anti-FLAG antibody indicates that even those ST cells displaying high nuclear ELF5 simultaneously display cytoplasmic CGB and ENDOU (Fig. 25E, F). Taken together, these results indicate that, similarly to the previously described ELF5 KD and ELF5 cOX lines, perturbed ELF5 levels in the ELF5 iOX line do not cause a loss of self-renewal or differentiation potential.

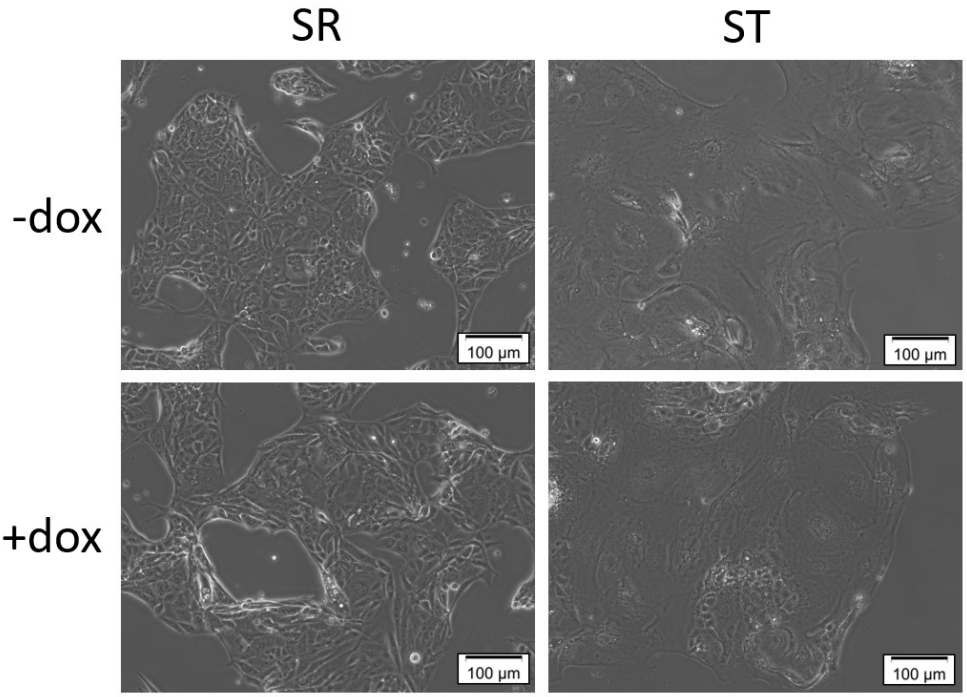

Figure 24. Brightfield microscopy images of the ELF5 iOX line with and without doxycycline (dox) under SR and upon differentiation to ST.
Cell morphologies are identical between the two cell lines in both states, indicating a null or minimal effect of the induction of ELF5 overexpression by dox.

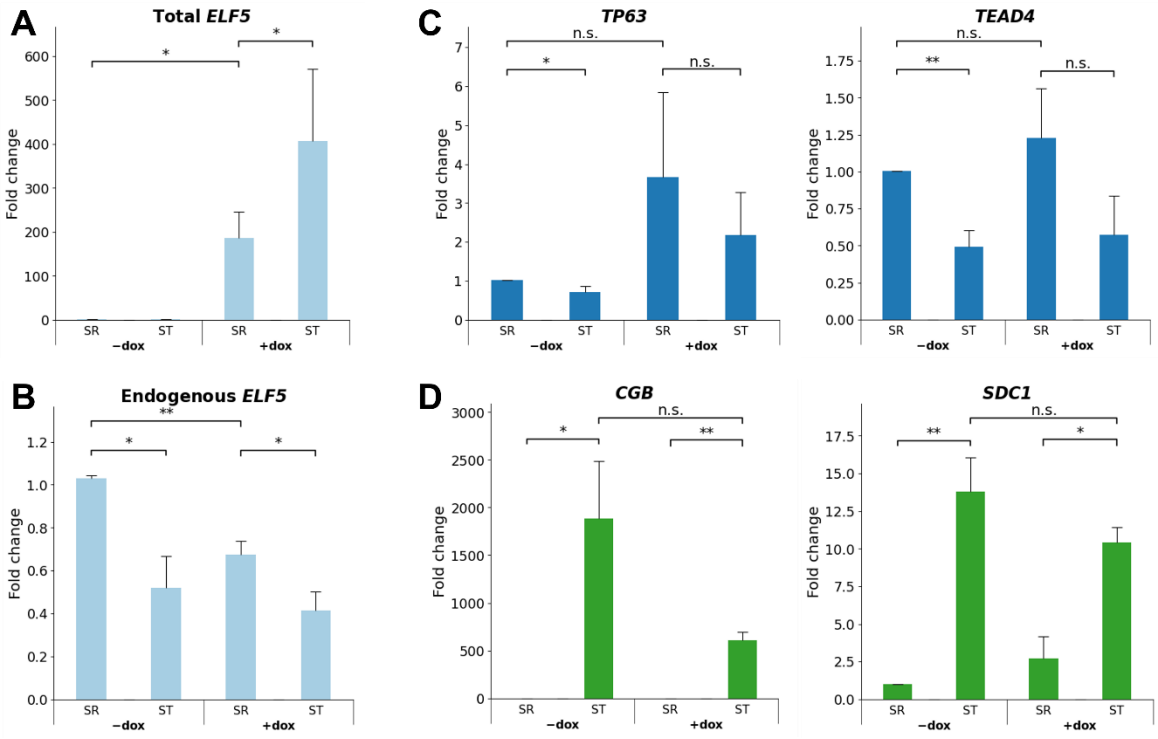

Legend on next page.

Figure 25. RT-qPCR analysis of the ELF5 iOX line under SR and upon differentiation to ST.
(A) Upon dox treatment, total *ELF5* levels are upregulated around 200-fold. (B) Endogenous *ELF5* levels decrease upon overexpression as compensation and decrease upon differentiation both in the absence and presence of dox. (C) *TP63* and *TEAD4* are not significantly downregulated upon differentiation under dox treatment. (D) *CGB* and *SDC1* are upregulated upon differentiation under both conditions, although the fold change is slightly smaller in the presence of dox. Error bars show S.E.M. for 3 biological replicates, with 3 technical replicates each. *p<0.1, **p<0.01, ***p<0.001

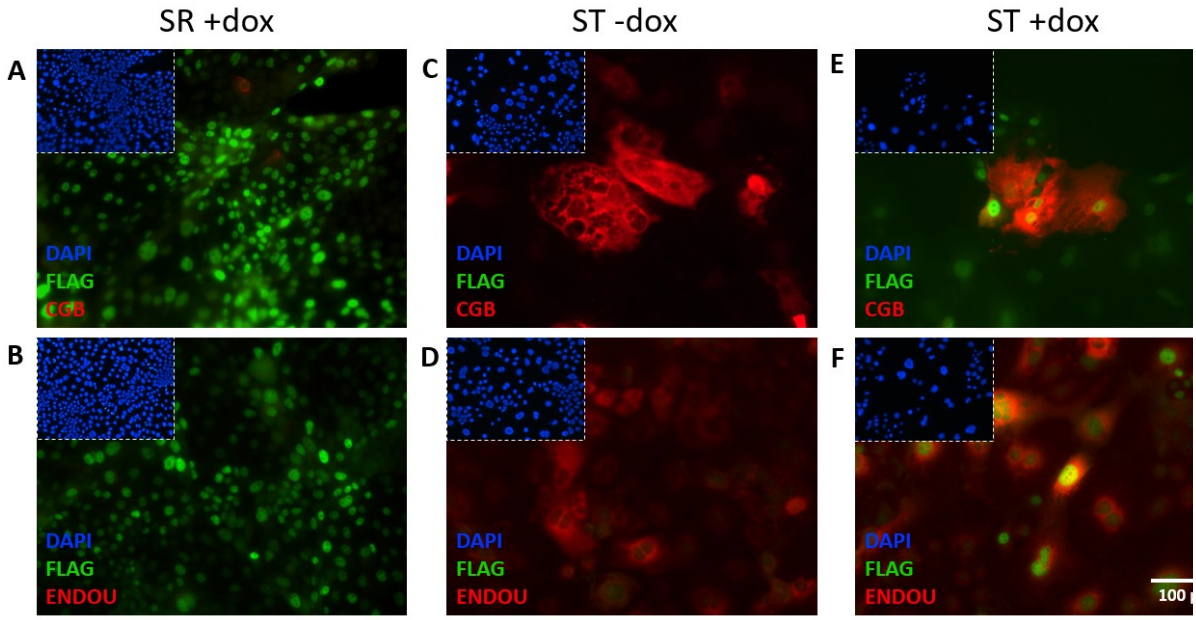

Figure 26. Immunofluorescence staining of the ELF5 iOX line under SR and upon differentiation to STs.
The ST markers (A) CGB and (B) ENDOU are not present under self-renewal. The detection of cytoplasmic (C) CGB and (D) ENDOU confirms differentiation to STs in the -dox control. The detection of cytoplasmic (E) CGB and (F) ENDOU confirms differentiation to STs upon induction of ELF5 overexpression by 48h dox treatment, which is confirmed by FLAG. DAPI is used as a nuclear marker.

5.6. Trophoblast organoids as an alternative model system

3D culture of hTSCs, resulting in trophoblast organoids (TB-ORGs), is a more physiologically relevant model system than 2D culture, due to spontaneous inner fusion into STs under self-renewal conditions. Thus, as previous results showed minimal disruption to directed ST differentiation by ELF5 overexpression, TB-ORGs were generated from the ELF5 iOX cell line to evaluate any potential disturbance to spontaneous ST differentiation. The TB-ORGs were grown for 14 days from the time that single cells were embedded in Matrigel domes, either in the

absence or sustained presence of dox. TB-ORGs were also generated from the empty vector control line in the presence of dox to control for any effects of this molecule on organoid formation and growth.

The effects of dox-induced ELF5 overexpression can clearly be observed as a hindered growth of TB-ORGs compared to the control (Fig. 27). Fewer of the single cells seeded formed TB-ORGs, and none of these reached the size of the control after 14 days of growth. This suggests a reduced ability of ELF5-overexpressing cells to proliferate in 3D and to spontaneously adopt the TB-ORG structure, with self-renewing CTB-like cells on the outside and fusion into STs on the inside.

This effect was quantitatively validated by performing RT-qPCR analysis on harvested organoids, following the same protocol as for 2D culture, in order to monitor the expression levels of key ST markers. First, the dox-induced expression of ectopic ELF5 was confirmed (Fig. 28A), and a compensatory downregulation of endogenous ELF5 similar to previous overexpression experiments was observed (Fig. 28B). In addition to *CGB* and *SDC1*, the ST markers *GCM1* and *ERVW1* were also analysed to obtain a more complete and reliable identification of ST identity. These four ST markers all display lower expression levels upon ELF5 overexpression compared to the -dox control, with up to an almost 60% decrease for *CGB* (Fig. 28C). Thus, these results indicate a hindered spontaneous differentiation to STs in ELF5-overexpressing TB-ORGs.

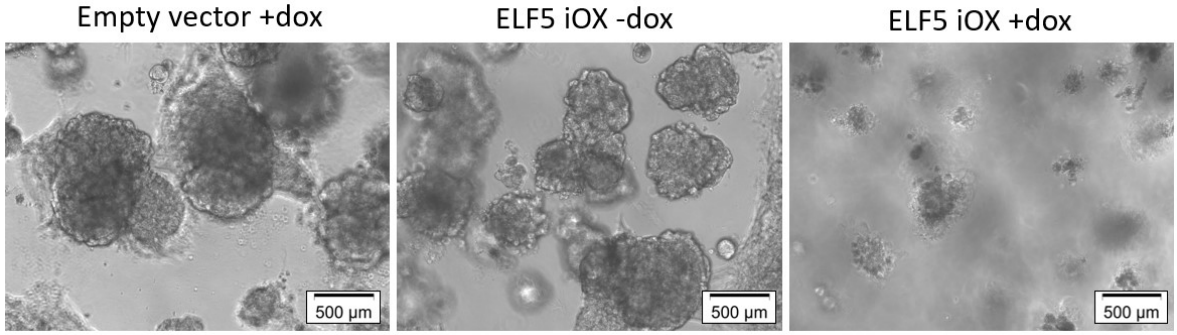

Figure 27. Brightfield microscopy images of ELF5 iOX TB-ORGs.
TB-ORGs were grown for 14 days from the time of embedding, and an empty vector control was used to monitor the effects of dox on growth. It can clearly be seen that the ELF5 iOX TB-ORGs with ELF5 overexpression induced by dox did not grow as large and many of the cells died.

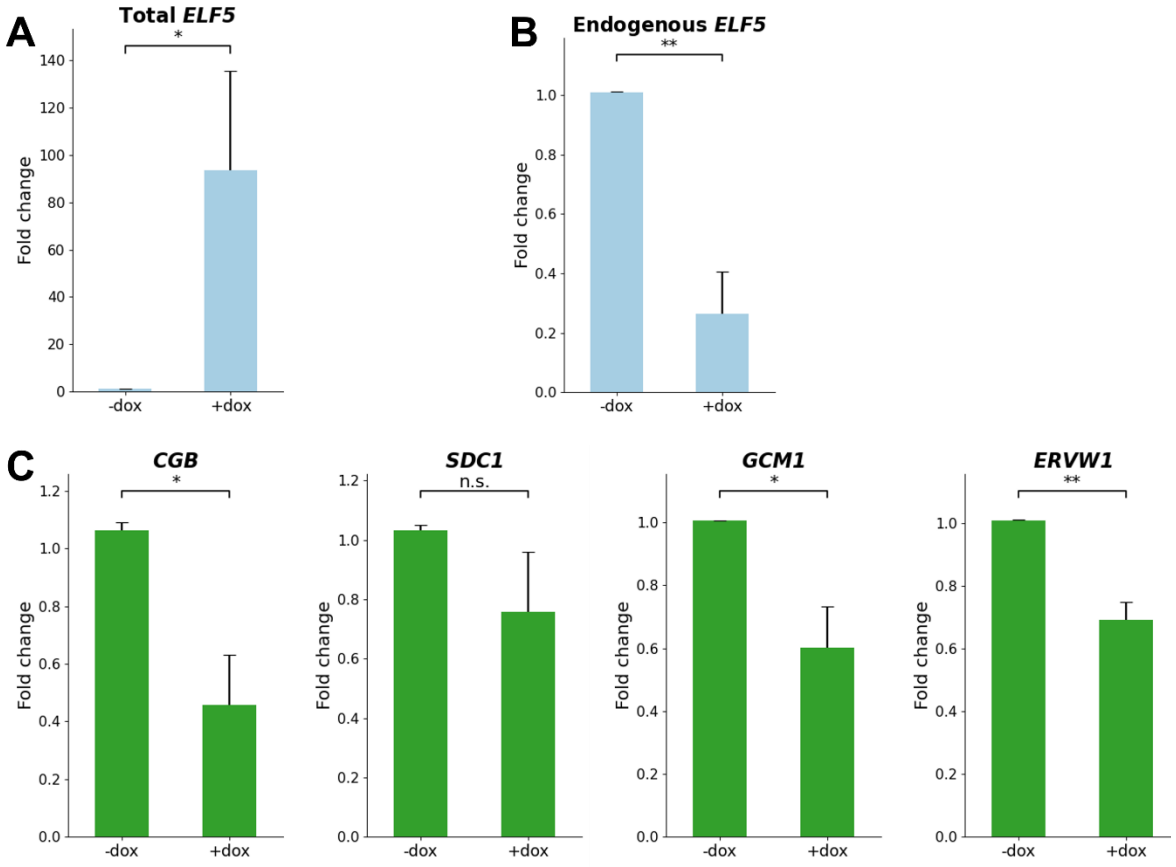

Figure 28. RT-qPCR analysis of ELF5 iOX TB-ORGs in the absence and presence of dox.
(A) ELF5 is successfully induced in TB-ORGs cultured in the presence of dox, causing an increase of around 100-fold. (B) For those TB-ORGs cultured in the presence of dox in which *ELF5* overexpression is induced, endogenous *ELF5* is downregulated in compensation. (C) The ST markers *CGB*, *GCM1* and *ERVW1* are all expressed at significantly lower levels in the presence of dox than in the control. This indicates a partial failure of the cells to undergo spontaneous syncytialisation. Error bars show S.E.M. for 3 biological replicates, with 3 technical replicates each. *p<0.1, **p<0.01, ***p<0.001

5.7. Generation of an ELF5-V5 and ELF5-EYFP line

A hTSC line with a V5 epitope tag on the endogenous *ELF5* locus was generated to provide an alternative to anti-ELF5 antibodies for the detection of ELF5 at the protein level, to be used in experimental applications such as immunofluorescence and Western blots, as anti-V5 antibodies are highly specific and readily available. This was carried out early on due to the anti-ELF5 antibody previously used in our lab (Santa Cruz Biotechnology, Catalogue Number sc-9645) being discontinued. We therefore had an initial lack of reliable antibody until an alternative was validated

(Thermo Fischer, Catalogue Number 720380). Additionally, an ELF5-V5 line will open future opportunities for functional analyses, such as co-immunoprecipitation to identify binding partners, at physiologically relevant ELF5 levels.

The V5 sequence was knocked-in at the C-terminus of endogenous *ELF5* using a CRISPR-Cas9 pipeline (Dewari et al., 2018) in which the cells are co-transfected with the Cas9 protein pre-complexed with a synthetic guide RNA (annealed tracrRNA and crRNA) and a single-stranded oligodeoxynucleotide (ssODN) repair template. The gRNA targets the 3'UTR of *ELF5* and the ssODN inserts the 42-nt V5 sequence between exon 6 and the STOP codon, using homologous recombination mediated by its 75-nt homology arms (HAs) (Fig. 29). Nucleofection of hTSCs was achieved by electroporation, with an efficiency of ~80% after 24 hours, as observed for the DsRed control electroporation that was performed in parallel. The V5 knock-in was first confirmed by genotyping the resulting cells in bulk, using PCR primers located in the V5 sequence and 3'UTR. Clonal cell populations were then obtained by limiting dilution of a cell suspension onto a 96-well plate, targeting a density of 0.5 cells/well to isolate single cells. Once these were expanded to an appropriate size, they were once again genotyped individually by PCR. In total, 20 clones were expanded and genotyped, and 6 clones showed positive genotyping results (Fig. 30). These 6 clones were all further analysed by Sanger sequencing, which confirmed the correct insertion of the V5 tag in two of them (Fig. 29). Both clonal cell populations were further expanded and stored at -80°C for future use.

Due to the potentially low endogenous ELF5 levels detected in the ELF5-iOX immunofluorescence experiment (Fig. 22) and the heterogeneity of its expression *in vivo* (Fig. 7), obtaining a reporter line is particularly interesting for hTSCs, as it would allow for the fast and easy detection of the ELF5 protein in live cells using fluorescence. Here, enhanced yellow fluorescent protein (EYFP) was fused to the C-terminus of the endogenous *ELF5* locus using the previously established Precise Integration into Target Chromosomes (PITCh) system (Brand and Winter, 2019), which is based on co-transfection with two plasmids. Firstly, the repair vector

contains the insertion cassette (EYFP and NeoR) flanked by 20 bp microhomology arms and gRNA target sites. Secondly, the cutting vector constitutively expresses Cas9 and two gRNAs targeting the 3'UTR of *ELF5* (the same insertion site as for the ELF5-V5 knock-in) and the gRNA targets sites of the cutting vector respectively (Fig. 31). Following co-transfection by electroporation, hTSCs were first selected for the presence of the transgene with Neomycin, and a knock-in was then confirmed in the bulk of these cells by PCR. The resulting agarose gel shows that some of the cells underwent a successful knock-in of EYFP (Fig. 32). Due to time constraints, the correct insertion of EYFP in the 3'UTR could not be further validated by sequencing clonal cell populations, which would need to be carried out in future experiments.

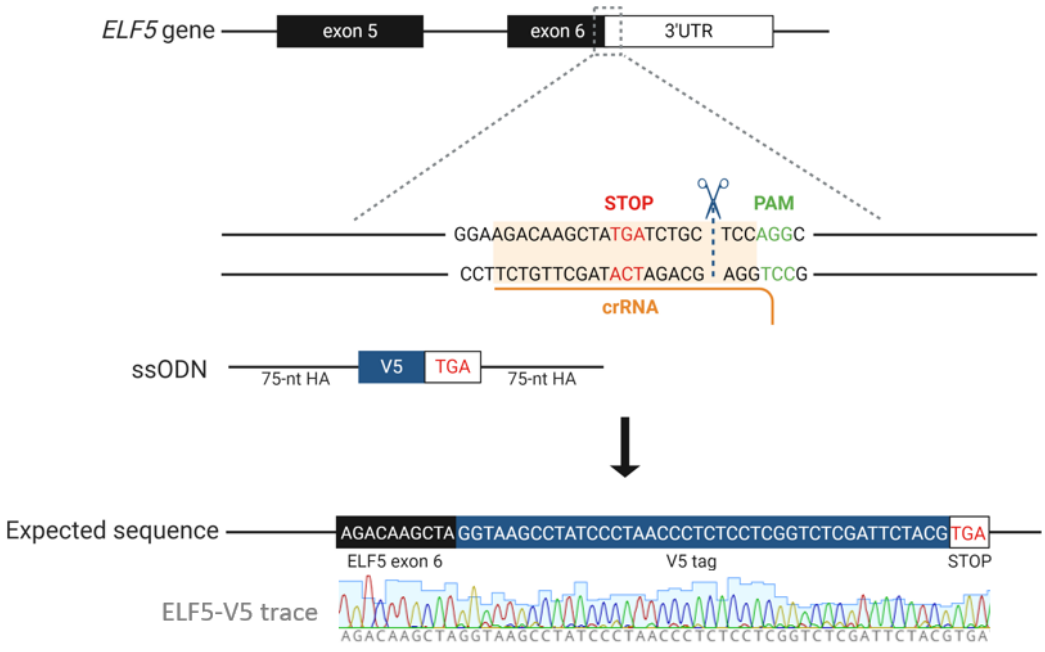

Figure 29. Schematic of the ELF5-V5 line generation by CRISPR-Cas9.
The crRNA was designed to target the 3' end of exon 6, and the ssODN repair template was designed to introduce the V5 sequence followed by the stop codon TGA. The sequence of the V5 tag and homology arms was confirmed by Sanger sequencing of the resulting hTSC line.

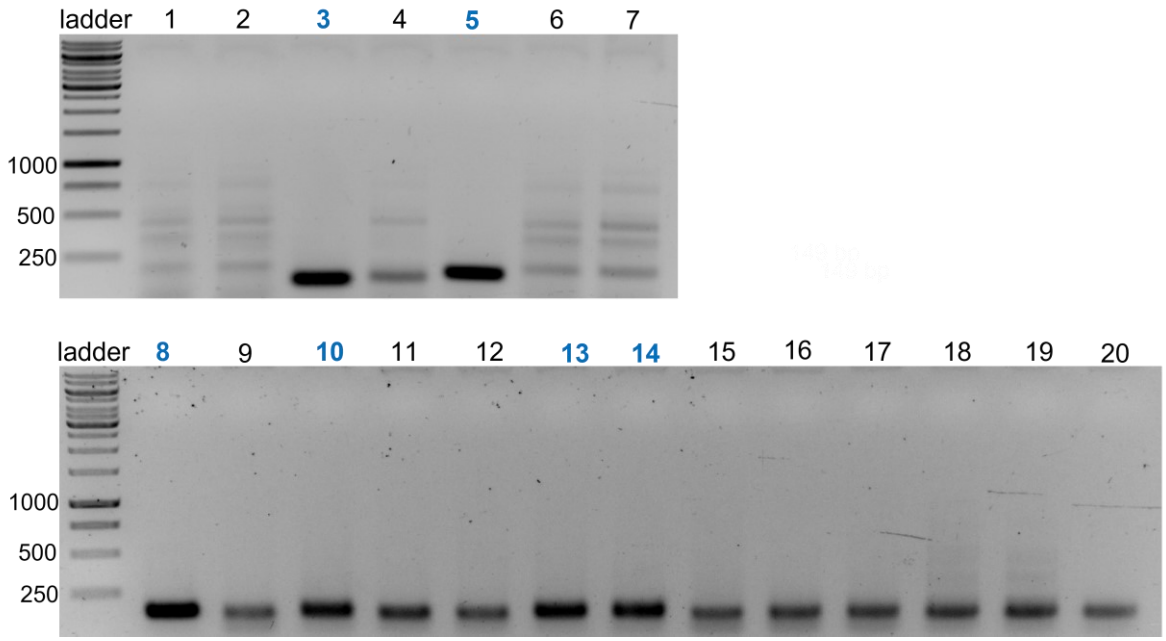

Figure 30. Genotyping of ELF5-V5 clones by PCR.
PCR primers were designed to target the V5 sequence and the 3'UTR of *ELF5*, and to produce a 149 bp amplicon if the V5 tag had successfully been knocked in. 20 clones were genotyped in total, and clones 3, 5, 8, 10, 13 and 14 (highlighted here in blue) were further analysed by Sanger sequencing because they showed the expected 149 bp band.

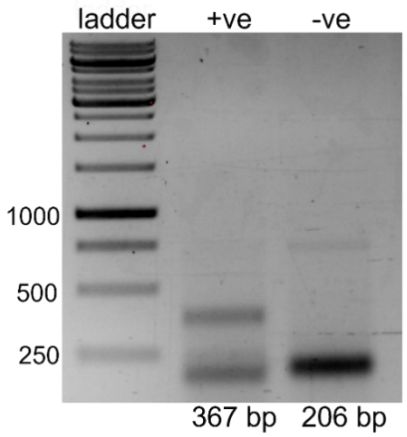

Figure 32. Bulk genotyping of the ELF5-EYFP knock-in by PCR.
Two sets of PCR primer pairs were designed to target the *EYFP* sequence and the 3'UTR of *ELF5*. One set produces a 367 bp amplicon upon the successful insertion of *EYFP* (+ve), while the other set produces a 206 bp amplicon if *EYFP* was not inserted (-ve). A clear band can be seen at 206 bp for negative events, as well as a clear band at 367 bp for positive events, indicating a successful knock-in in some cells.

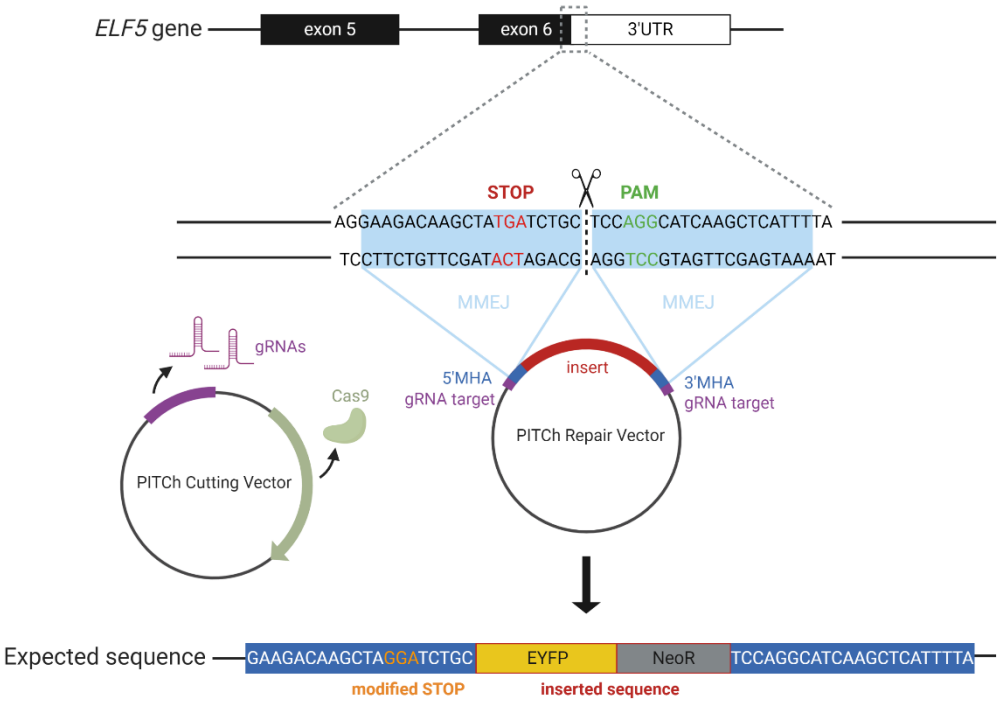

Figure 31. Schematic of the ELF5-EYFP reporter line generation by the PITCh system.
The PITCh Cutting and Repair vectors were introduced into the cells simultaneously to insert the cassette containing the *EYFP* CDS and the neomycin resistance gene at the 3' end of exon 6. The *ELF5* STOP codon was modified in the 5' microhomology arm to allow for continuous transcription and for the production of a fusion protein.

6. Discussion

ELF5 is a hallmark of trophoblast, and its expression is epigenetically restricted to the CTB progenitor cells of the developing human placenta, which is why hypomethylation of the *ELF5* promoter has previously been selected as a key criterion for defining *in vitro* human trophoblast (Hemberger et al., 2010, Lee et al., 2016). The initial immunofluorescence staining carried out here on placental sections confirmed the presence of ELF5 in the CTB layer of chorionic villi, and conforming to this, analysis of *ELF5* expression in hTSCs showed downregulation upon directed differentiation towards STs and EVTs. Thus, it was hypothesized that ELF5 could act as a master transcription factor regulating hTSC differentiation and self-renewal. This was tested by perturbing ELF5 levels in hTSCs and observing the effects of this on hTSCs in both the self-renewal state and upon differentiation to STs. An

shRNA knock-down was generated, as well as constitutive and induced overexpression. In each case, these hTSC lines morphologically resembled the control hTSCs and maintained their ability to differentiate into STs, which was quantitatively validated by RT-qPCR and immunofluorescence assays of the key ST markers CGB, SDC1 and ENDOU. These results contrast with those of previous studies performed on murine TSCs, which found that both Elf5 knockdown and overexpression cause their precocious differentiation (Pearton et al., 2014, Latos et al., 2015). The fact that the same effect is not observed for human ELF5 reflects how, despite their equivalent functions, human and murine placentas make use of different transcription factor networks that only partially overlap (Soncin et al., 2018).

There is strong evidence for different regulatory networks being responsible for proper mouse and human placentation respectively. Fundamental morphological differences such as gestational length, litter size, and organization of trophoblast cell types within the placenta are supported by molecular differences in early development (Soncin et al., 2015). This begins in the pre-implantation embryo, for which single-cell RNA sequencing showed that *ELF5* and *EOMES* are present in mice but absent in humans (Blakeley et al., 2015). Post-implantation development in humans also lacks *EOMES* expression (Soncin et al. 2018), which rules out the well-characterised Eomes-Elf5-Tfap2c transcription factor network regulating the balance between murine TSC self-renewal and differentiation (Latos et al., 2015). There is also an increasing number of known human-specific placental proteins, one important example being the MHC Class I molecule HLA-G, which is crucial for trophoblast invasion (Schmidt et al., 2015). These interspecies differences between placental progenitors can lead us to question the value of the mouse model in investigating the development of diseases. For instance, there have been various attempts to model the human-specific disease preeclampsia in mice, using methods such as the administration of exogenous agents to pregnant mice to induce similar

pathologies. However, the resulting phenotypes are often inconsistent and inaccurate (Waker et al., 2021), once again highlighting the need for a human model.

When using *in vitro* systems to model processes as complex as placentation, the physiological relevance of the model should be carefully considered. Compared to primary CT cells, all CT markers examined in hTSCs by Okae and colleagues exhibit the expected expression patterns, however some genes including *LRP5*, *TP63* and *ELF5* show lower expression levels in hTSCs (Okae et al., 2018). This reflects how the *in vitro* conditions may slightly alter the transcriptome, and the low ELF5 levels in hTSCs was confirmed here in the immunofluorescence experiments performed on the ELF5_iOX line, where the anti-ELF5 antibody was only detected upon induction by dox. Furthermore, the observation made here that ELF5_OX and ELF5_iOX cells compensate for ectopic ELF5 by downregulating endogenous expression indicates that the hTSC culture conditions may be incompatible with high levels of ELF5. The experiments performed on TB-ORGs suggested that these are more sensitive to disrupted ELF5 levels than hTSCs in 2D culture, and hence may be a more accurate model system to be used in the future.

Another significant observation is that *ELF5* appears to be expressed highly only in a small subset of CTBs. The immunofluorescence staining performed on first trimester placenta sections showed that although restricted to the CTB layer, ELF5 protein was not detected at constant levels within these cells, and the protein was found to be present at lower levels at 10 weeks than at 7 weeks. This was also shown previously in the data resulting from single cell sequencing of the human first trimester placenta (Liu et al., 2018), which revealed a very heterogenous CTB population. Indeed, most cells displayed an FPKM value of 0 for *ELF5* and the correlation between the expression level of *ELF5* and the CTB markers *TP63* and *TEAD4* was very low. Furthermore, *in situ* hybridisation experiments previously performed suggest a similar heterogeneity, with *ELF5* being co-expressed with *CDX2* in only a subset of CTBs, and a downregulation of *ELF5* expression as gestation progresses (Soncin et al., 2018).

Taking all these elements into account, it may be the case that hTSCs do not truly represent an *in vivo* stem cell equivalent, but rather a less multipotent progenitor population with, among other differences, lower *ELF5* expression levels than primary CTBs. Such progenitors may be found *in vivo* and correspond to a CTB subpopulation that is housed in a specific niche of the developing placenta later in gestation. Indeed, some CTBs have been found to persist until the end of pregnancy (Mori et al., 2007). Throughout the stages of blastocyst implantation at E6-7, beginning of placental development at E8, establishment of the mother-fetus vascular connection by week 12 and expanding vasculature in the second trimester, CTBs may transition through states of decreasing potency and proliferation. Thus, hTSCs could correspond to a late first trimester or second trimester CTB state, which would explain their low levels of *ELF5* expression. On the other hand, hTSCs may simply be CTBs of the early post-implantation trophoblast that have adapted to *in vitro* conditions, and in this case, they would not represent a physiologically relevant subpopulation. It is important to remember that trophoblasts *in vivo* do not differentiate in isolation, but among cells of the villous core originating from the ExM. This is a very different environment than the one provided *in vitro*, suggesting that cells must undergo adaptation to a certain extent.

In order to open new avenues for functional experiments on the role of ELF5, a V5 epitope tag was successfully introduced into the endogenous locus. This will provide a means for highly sensitive detection when investigating protein levels and subcellular location, as well as for identification of its biochemical interactors in pull-down assays. Furthermore, a fluorescent knock-in reporter system for the live detection of endogenous ELF5 in hTSCs through the expression of EYFP was generated, enabling its quick and easy quantification across culture conditions. Combining this assay with high-throughput screening of chemical libraries, putative small compound regulators could be identified that influence expression levels and thus cell identity. In the future, this could be used to optimise the current hTSC medium to obtain a model system that more faithfully replicates the *in vivo* state, with

elevated *ELF5* expression levels. If the current hTSC model does represent CTBs from a later developmental stage, it should be possible to obtain a hTSC state that corresponds to an earlier developmental stage, using *ELF5* expression as a readout. This could be achieved by modifying the culture conditions, analogously to the conversion of primed hESCs into naïve hESCs under NHSM (naïve human stem cell medium) conditions (Gafni et al., 2014). Optimizing the hTSC model in this way will be instrumental in achieving novel molecular insights into the importance of ELF5 in trophoblast self-renewal and differentiation and the elucidation of its mode of action.

While hTSCs are a key focus in the field, these cells may nevertheless remain of limited value due to the ethical and legal challenges against their use and their unknown disease potential (Horii et al., 2020). As previously mentioned, the hTSC model requires prolonged culture, which may lead to adaptations to *in vitro* conditions and therefore mask the differences between healthy and pathological tissue. A more recent alternative is the derivation of hTSCs from induced pluripotent stem cells (iPSCs) (Gaël et al., 2020). These would solve the restricted accessibility of placental samples from early gestation, increase the genetic diversity of existing cell lines and provide models of validated normal and pathological development. Another promising advance was the recent derivation of blastoids (blastocyst-like structures) from naïve human iPSCs, which involved the induction of a TE lineage corresponding to a very early developmental stage (E5-7). This was achieved by exposing iPSCs to lysophosphatidic acid (LPA) (a Hippo pathway inhibitor), A83-01 (a TGFβ receptor inhibitor) and PD0325901 (an ERK inhibitor) in a medium containing the STAT activator leukaemia inhibitory factor (LIF) and Y-27632 (a ROCK inhibitor) (Kagawa et al., 2021). These conditions differ from the hTSC conditions used here by the addition of LPA, PD0325901 and LIF, and hence could perhaps be used to derive more naïve hTSCs than the current model.

The future perspectives of the field will involve refining the establishment of such trophoblast cell lines and determining exactly which timepoint of placental

development they replicate. Regarding ELF5, it will be important to determine whether its expression levels are indeed an indication of developmental stage, or if human ELF5 is generally a less crucial factor in trophoblast development than its murine counterpart. Subsequently, pregnancy complications caused by the failure of trophoblast growth and differentiation could be more accurately modelled *in vitro* by establishing 2D hTSC cultures or 3D TB-ORGs from iPSCs of patients. Considering the crucial role of the placenta in pregnancy complications and long-term health, better insights into the molecular mechanisms of early placental development will advance the available therapeutic treatment of pregnancy pathologies. For instance, various placental disorders could be classified according to cellular criteria, to narrow the focus on which molecular pathways to test (Maltepe et al., 2010). ELF5 function in the placenta may also be translatable into other organ systems where it is expressed, such as breast tissue, which is particularly susceptible to an imbalance between cell proliferation and differentiation leading to cancer. Hence, understanding the mechanism of ELF5 function may contribute to establishing a paradigm for the pathways that ensure not only normal development but also health throughout adult life.

7. References

Abou-Kheir, W., Barrak, J., Hadadeh, O., Daoud, G. (2017). HTR-8/SVneo cell line contains a mixed population of cells. *Placenta*, *50*, 1–7.

Amita, M., Adachi, K., Alexenko, A. P., Sinha, S., Schust, D. J., Schulz, L. C., Roberts, R. M., Ezashi, T. (2013). Complete and unidirectional conversion of human embryonic stem cells to trophoblast by BMP4. *Proceedings of the National Academy of Sciences of the United States of America*, *110*(13).

Blakeley, P., Fogarty, N. M. E., Valle, I., Wamaitha, S. E., Hu, T. X., Elder, K., Snell, P., Christie, L., Robson, P., Niakan, K. K., Blakeley, P., Fogarty, N. M. E., Valle, I., Wamaitha, S. E., Hu, T. X., Elder, K., Snell, P., Christie, L., Robson, P., Niakan, K. K. (2015). Erratum to Defining the three cell lineages of the human blastocyst by single-cell RNA-seq. *Development, 142*, 3151-3165.

Brand, M., & Winter, G. E. (2019). Locus-Specific Knock-In of a Degradable Tag for Target Validation Studies. *Target Identification and Validation in Drug Discovery: Methods and Protocols, 1953*, 105–119.

Brosens, I., Pijnenborg, R., Vercruysse, L., Romero, R. (2011) The "Great Obstetrical Syndromes" are associated with disorders of deep placentation. *Am J Obstet Gynecol, 204*, 193–201.

Cheong, M. L., Wang, L. J., Chuang, P. Y., Chang, C. W., Lee, Y. S., Lo, H. F., Tsai, M. S., Chen, H. (2015). A positive feedback loop between glial cells missing 1 (GCM1) and human chorionic gonadotropin (hCG) regulates placental hCGβ expression and cell differentiation. *Molecular and Cellular Biology*, *36*(1), 197-209.

Cierna, Z., Varga, I., Danihel, L., Kuracinova, K., Janegova, A., Danihel, L. (2016). Intermediate trophoblast-distinctive, unique and often unrecognized population of trophoblastic cells. *Annals of Anatomy*, *204*, 45–50.

Cinkornpumin, J. K., Kwon, S. Y., Guo, Y., Hossain, I., Sirois, J., Russett, C. S., Tseng, H.-W., Okae, H., Arima, T., Duchaine, T. F., Liu, W., Pastor, W. A. (2020). Stem Cell Reports Article Naive Human Embryonic Stem Cells Can Give Rise to Cells with a Trophoblast-like Transcriptome and Methylome. *Stem Cell Reports, 15*, 198-213.

Dasilva-Arnold, S., James, J. L., Al-Khan, A., Zamudio, S., Illsley, N. P. (2015). Differentiation of first trimester cytotrophoblast to extravillous trophoblast involves an epithelial-mesenchymal transition. *Placenta*, *36*(12), 1412–1418.

Davies, J., Pollheimer, J., Yong, H. E. J., Kokkinos, M. I., Kalionis, B., Knöfler, M., Murthi, P. (2016). Epithelial-mesenchymal transition during extravillous trophoblast differentiation. *Cell Adhesion and Migration*, *10*(3), 310–321.

Dewari, P. S., Southgate, B., Mccarten, K., Monogarov, G., O'duibhir, E., Quinn, N., Tyrer, A., Leitner, M.-C., Plumb, C., Kalantzaki, M., Blin, C., Finch, R., Bressan, R. B., Morrison, G., Jacobi, A. M., Behlke, M. A., Von Kriegsheim, A., Tomlinson, S., Krijgsveld, J., Pollard, S. M. (2018). An

efficient and scalable pipeline for epitope tagging in mammalian stem cells using Cas9 ribonucleoprotein. *eLife, 7*, e35069

Donnison, M., Beaton, A., Davey, H. W., Broadhurst, R., L'Huillier, P., Pfeffer, P. L. (2005) Loss of the extraembryonic ectoderm in Elf5 mutants leads to defects in embryonic patterning. *Development*, *132*(10), 2299-308.

Frank, H. G., Gunawan, B., Ebeling-Stark, I., Schulten, H. J., Funayama, H., Cremer, U., Huppertz, B., Gaus, G., Kaufmann, P., Füzesi, L. (2000). Cytogenetic and DNA-fingerprint characterization of choriocarcinoma cell lines and a trophoblast /choriocarcinoma cell hybrid. *Cancer Genetics and Cytogenetics, 116*(1), 16–22.

Frend, H. T., & Watson, C. J. (2013). Elf5 - breast cancer's little helper. *Breast Cancer Research*, *15*(2), 1–2.

Gaël, C., Dimitri, M., Betty, B., Julie, F., Justine, B., Sophie, L., Alexandre, B., Simon, C., Stephanie, K., Caroline, C., Anne, G., Quentin, F., Harunobu, K., Eric, C., Léa, F., Valentin, F., Sandra, H., Bianca, D., Martin, K., Laurent, D. (2020). Generation of human induced trophoblast stem cells. *BioRxiv*, 2020.09.15.298257.

Gafni, O., Weinberger, L., Mansour, A. A., Manor, Y. S., Chomsky, E., Ben-Yosef, D., Kalma, Y., Viukov, S., Maza, I., Zviran, A., Rais, Y., Shipony, Z., Mukamel, Z., Krupalnik, V., Zerbib, M., Geula, S., Caspi, I., Schneir, D., Shwartz, T., Hanna, J. H. (2013). Derivation of novel human ground state naive pluripotent stem cells. *Nature*, *504*(7479), 282–286.

Gossen, M., Freundlieb, S., Bender, G., Müller, G., Hillen, W., Bujard, H. (1995) Transcriptional activation by tetracyclines in mammalian cells. *Science*, *268*(5218), 1766-9.

Graham, W., Woodd, S., Byass, P., Filippi, V., Gon, G., Virgo, S., Chou, D., Hounton, S., Lozano, R., Pattinson, R. (2016). Diversity and divergence: the dynamic burden of poor maternal health. *Lancet, 388,* 2164-2175.

Haider, S., Meinhardt, G., Saleh, L., Fiala, C., Pollheimer, J., Knöfler, M. (2016). Notch1 controls development of the extravillous trophoblast lineage in the human placenta. *PNAS, 13*(48), 7710-7719.

Haider, S., Meinhardt, G., Saleh, L., Kunihs, V., Gamperl, M., Kaindl, U., Ellinger, A., Burkard, T. R., Fiala, C., Pollheimer, J., Mendjan, S., Latos, P. A., Knöfler, M. (2018). Self-Renewing Trophoblast Organoids Recapitulate the Developmental Program of the Early Human Placenta. *Stem Cell Reports*, *11*(2), 537–551.

Heaton, S. J., Eady, J. J., Parker, M. L., Gotts, K. L., Dainty, J. R., Fairweather-Tait, S. J., McArdle, H. J., Srai, K. S., Elliott, R. M. (2008). The use of BeWo cells as an in vitro model for placental iron transport. *American Journal of Physiology - Cell Physiology*, *295*(5), C1445-C1453.

Hemberger, M., Hanna, C. W., Dean, W. (2019). Mechanisms of early placental development in mouse and humans. *Nature Reviews Genetics, 21,* 27-43.

Hemberger, M., Udayashankar, R., Tesar, P., Moore, H., Burton, G. J. (2010) ELF5-enforced transcriptional networks define an epigenetically regulated trophoblast stem cell compartment in the human placenta. *Human Molecular Genetics. 19*(12), 2456-2467.

Horii, M., Li, Y., Wakeland, A. K., Pizzo, D. P., Nelson, K. K., Sabatini, K. (2016). Human pluripotent stem cells as a model of trophoblast differentiation in both normal development and disease. *PNAS,* 3882-8391.

Horii, M., Touma, O., Bui, T., Parast, M. (2019). Modeling human trophoblast, the placental epithelium at the maternal fetal interface. *Reproduction, 160,* R1–R11.

Jokimaa, V., Inki, P., Kujari, H., Hirvonen, O., Ekholm, E., Anttila, L. (1998) Expression of syndecan-1 in human placenta and decidua. *Placenta*, *19*(2-3), 157-163.

Kagawa, H., Javali, A., Khoei, H. H., Sommer, T. M., Sestini, G., Novatchkova, M., Scholte op Reimer, Y., Castel, G., Bruneau, A., Maenhoudt, N., Lammers, J., Loubersac, S., Freour, T., Vankelecom, H., David, L., Rivron, N. (2021). Human blastoids model blastocyst development and implantation. *Nature*, *601*, 600–605.

Knöfler M, Vasicek R, Schreiber M (2001) Key regulatory transcription factors involved in placental trophoblast development—a review. *Placenta, 22*(Suppl A), S83–S92.

Knöfler, M., Haider, S., Saleh, L., Pollheimer, J., Gamage, T. K. J. B., James, J. (2019). Human placenta and trophoblast development: key molecular mechanisms and model systems. *Cellular and Molecular Life Sciences*, *76*(18), 3479–3496.

Krendl, C., Shaposhnikov, D., Rishko, V., Ori, C., Ziegenhain, C., Sass, S., Simon, L., Müller, N. S., Straub, T., Brooks, K. E., Chavez, S. L., Enard, W., Theis, F. J., Drukker, M. (2017). GATA2/3-TFAP2A/C transcription factor network couples human pluripotent stem cell differentiation to trophectoderm with repression of pluripotency. *Proc Natl Acad Sci USA*, *114*(45), E9579–E9588.

Kuckenberg, P., Kubaczka, C., Schorle, H. (2012). The role of transcription factor Tcfap2c/TFAP2C in trophectoderm development. *Reproductive BioMedicine Online*, *25*(1), 12–20.

Latos, P. A., & Hemberger, M. (2016). From the stem of the placental tree: Trophoblast stem cells and their progeny. *Development (Cambridge), 143*(20), 3650–3660.

Lee, C. Q. E., Gardner, L., Turco, M., Zhao, N., Murray, M. J., Coleman, N., Rossant, J., Hemberger, M., Moffett, A. (2016). What Is Trophoblast? A Combination of Criteria Define Human First-Trimester Trophoblast. *Stem Cell Reports, 6*(2), 257–272.

Li, Y., Moretto-Zita, M., Leon-Garcia, S., Parast, M. M. (2014). P63 inhibits extravillous trophoblast migration and maintains cells in a cytotrophoblast stem cell-like state. *American Journal of Pathology*, *184*(12), 3332–3343.

Liu, Y., Fan, X., Wang, R., Lu, X., Dang, Y. L., Wang, H., Lin, H. Y., Zhu, C., Ge, H., Cross, J. C., Wang, H. (2018). Single-cell RNA-seq reveals the diversity of trophoblast subtypes and patterns of differentiation in the human placenta. *Cell Research, 28*(8), 819–832.

Loregger T, Pollheimer J, Knöfler M (2003) Regulatory transcription factors controlling function and differentiation of human trophoblast—a review. *Placenta, 24*(Suppl A), S104–S110.

Maltepe, E., Bakardjiev, A. I., Fisher, S. J. (2010). The placenta: Transcriptional, epigenetic, and physiological integration during development. *Journal of Clinical Investigation*, *120*(4), 1016–1025.

Moffat, J., Grueneberg, D. A., Yang, X., Kim, S. Y., Kloepfer, A. M., Hinkle, G., Root, D. E. (2006). A Lentiviral RNAi Library for Human and Mouse Genes Applied to an Arrayed Viral High-Content Screen. *Cell*, *124*(6), 1283–1298.

Moffett, A., & Loke, C. (2006). Immunology of placentation in eutherian mammals. *Nature Reviews Immunology*, *6*(8), 584–594.

Mori, M., Ishikawa, G., Luo, S. S., Mishima, T., Goto, T., Robinson, J. M., Matsubara, S. Takeshita, T., Kataoka, H., Takizawa, T. (2007). The cytotrophoblast layer of human chorionic villi becomes thinner but maintains its structural integrity during gestation. *Biology of Reproduction*, *76*(1), 164–172.

Napso, T., Yong. H. E. J., Lopez Tello, J., Sferruzzi Perri, A. N. (2018) The role of placental hormones in mediating maternal adaptations to support pregnancy and lactation. *Front Physiol, 9*, 1091.

Niakan, K. K., & Eggan, K. (2013). Analysis of human embryos from zygote to blastocyst reveals distinct gene expression patterns relative to the mouse. *Developmental Biology*, *375*(1), 54–64.

Niakan, K. K., Han, J., Pedersen, R. A., Simon, C., Pera, R. A. R. (2012). Human pre-implantation embryo development. *Development*, *139*(5), 829–841.

Ng, R. K., Dean, W., Dawson, C., Lucifero, D., Madeja, Z., Reik, W., Hemberger, M. (2008). Epigenetic restriction of embryonic cell lineage fate by methylation of Elf5. *Nature Cell Biology, 10*(11), 1280–1290.

Okae, H., Toh, H., Sato, T., Hiura, H., Takahashi, S., Shirane, K., Kabayama, Y., Suyama, M., Sasaki, H., Arima, T. (2018) Derivation of Human Trophoblast Stem Cells. *Cell Stem Cell. 22*(1), 50-63.

Orendi, K., Kivity, V., Sammar, M., Grimpel, Y., Gonen, R., Meiri, H., Lubzens, E., Huppertz, B. (2011). Placental and trophoblastic in vitro models to study preventive and therapeutic agents for preeclampsia. *Placenta*, *32*(SUPPL. 1), S49–S54.

Paul, S., Home, P., Bhattacharya, B., Ray, S. (2017). GATA factors: Master regulators of gene expression in trophoblast progenitors. *Placenta*, *60*, S61–S66.

Pearton, D. J., Smith, C. S., Redgate, E., van Leeuwen, J., Donnison, M., Pfeffer, P. L. (2014). Elf5 counteracts precocious trophoblast differentiation by maintaining Sox2 and 3 and inhibiting Hand1 expression. *Developmental Biology*, *392*(2), 344–357.

Piggin, C. L., Roden, D. L., Gallego-Ortega, D., Lee, H. J., Oakes, S. R., Ormandy, C. J. (2016). ELF5 isoform expression is tissue-specific and significantly altered in cancer. *Breast Cancer Research*, *18*(1), 1–18.

Pollheimer, J., Vondra, S., Baltayeva, J., Beristain, A. G., Knöfler, M. (2018). Regulation of placental extravillous trophoblasts by the maternal uterine environment. *Frontiers in Immunology*, *9*, 1–18.

Roberts, R. M., Loh, K. M., Amita, M., Bernardo, A. S., Adachi, K., Alexenko, A. P., Schust, D. J., Schulz, L. C., Telugu, B. P. V. L., Ezashi, T., Pedersen, R. A. (2014). Differentiation of trophoblast cells from human embryonic stem cells: To be or not to be? *Reproduction, 147*(5), D1-D12.

Saha, B., Ganguly, A., Home, P., Bhattacharya, B., Ray, S., Ghosh, A., Karim Rumi, M. A., Marsh, C., French, V. A., Gunewardena, S., Paul, S. (2020). TEAD4 ensures postimplantation development by promoting trophoblast self-renewal: An implication in early human pregnancy loss. *Proc Natl Acad Sci USA*, *117*(30), 17864–17875.

Schmidt, A., Morales-Prieto, D. M., Pastuschek, J., Fröhlich, K., Markert, U. R. (2015). Only humans have human placentas: Molecular differences between mice and humans. *Journal of Reproductive Immunology*, *108*, 65–71.

Singh Dewari, P., Southgate, B., Mccarten, K., Monogarov, G., O'duibhir, E., Quinn, N., Tyrer, A., Leitner, M.-C., Plumb, C., Kalantzaki, M., Blin, C., Finch, R., Bressan, R. B., Morrison, G., Jacobi, A. M., Behlke, M. A., Von Kriegsheim, A., Tomlinson, S., Krijgsveld, J., Pollard, S. M. (2018). An efficient and scalable pipeline for epitope tagging in mammalian stem cells using Cas9 ribonucleoprotein. *eLife, 7,* e35069.

Singh, A. M. (2019) An Efficient Protocol for Single-Cell Cloning Human Pluripotent Stem Cells. *Frontiers in Cell and Developmental Biology, 7*, 11.

Smith, G. C. (2012) First-trimester determination of complications of late pregnancy. *J. Am. Med. Assoc., 303*, 561–562.

Soncin, F., Khater, M., To, C., Pizzo, D., Farah, O., Wakeland, A., Rajan, K. A. N., Nelson, K. K., Chang, C. W., Moretto-Zita, M., Natale, D. R., Laurent, L. C., Parast, M. M. (2018). Comparative analysis of mouse and human placentae across gestation reveals species-specific regulators of placental development. *Development (Cambridge)*, *145*(2), 1-13.

Soncin, F., Natale, D., Parast, M. M. (2015). Signaling pathways in mouse and human trophoblast differentiation: A comparative review. *Cellular and Molecular Life Sciences*, *72*(7), 1291–1302.

Speeg, K. V. (1979). Stimulation of Human Chorionic Gonadotropin by JAr Line Choriocarcinoma after Inhibition of DNA Synthesis. *Cancer Research*, *39*, 1952–1959.

Stromberg, K., Azizkhan, J., C., Speeg, K. V. (1978). Isolation of functional human trophoblast cells and their partial characterization in primary cell culture. *In Vitro, 14*, 631–638.

Tanaka S, Kunath T, Hadjantonakis A-K, Nagy A, Rossant J. (1998). Promotion of trophoblast stem cell proliferation by FGF4. *Science*, *282*, 2072– 2075.

Teasdale, F. & Jean-Jacques, G. (1985) Morphometric evaluation of the microvillous surface enlargement factor in the human placenta from mid-gestation to term. *Placenta*, *6(5),* 375-381.

Tersigni, C., Meli, F., Neri, C., Iacoangeli, A., Franco, R., Lanzone, A., Scambia, G., Di Simone, N. (2020). Role of human leukocyte antigens at the feto-maternal interface in normal and pathological pregnancy: An update. *International Journal of Molecular Sciences*, *21*(13), 1–13.

Turco, M. Y., Gardner, L., Kay, R. G., Hamilton, R. S., Prater, M., Hollinshead, M. S., McWhinnie, A., Esposito, L., Fernando, R., Skelton, H., Reimann, F., Gribble, F. M., Sharkey, A., Marsh, S. G. E., O'rahilly, S., Hemberger, M., Burton, G. J., Moffett, A. (2018). Trophoblast organoids as a model for maternal–fetal interactions during human placentation. *Nature, 564*(7735), 263–281.

Turco, M. Y., Moffett, A. (2019). Development of the human placenta. *Development (Cambridge), 146(*22), 1-14.

Velicky, P., Knöfler, M., Pollheimer, J. (2016). Function and control of human invasive trophoblast subtypes: Intrinsic vs. maternal control. *Cell Adhesion and Migration*, *10*(1–2), 154–162.

Waker, C. A., Kaufman, M. R., Brown, T. L. (2021). Current State of Preeclampsia Mouse Models: Approaches, Relevance, and Standardization. *Frontiers in Physiology*, *12*, 681632.

Weiss, G., Sundl, M., Glasner, A., Huppertz, B., Moser, G. (2016). The trophoblast plug during early pregnancy: a deeper insight. *Histochemistry and Cell Biology*, *146*(6), 749–756.

Zdravkovic, T., Nazor, K. L., Larocque, N., Gormley, M., Donne, M., Hunkapillar, N., Giritharan, G., Bernstein, H. S., Wei, G., Hebrok, M., Zeng, X., Genbacev, O., Mattis, A., Mcmaster, M. T. (2015). Human stem cells from single blastomeres reveal pathways of embryonic or trophoblast fate specification. *Development, 142*, 4010–4025.

Zhou, J., Chehab, R., Tkalcevic, J., Naylor, M. J., Harris, J., Wilson, T. J., Tsao, S., Tellis, I., Zavarsek, S., Xu, D., Lapinskas, E. J., Visvader, J., Lindeman, G. J., Thomas, R., Ormandy, C. J., Hertzog, P. J., Kola, I., Pritchard, M. A. (2005). Elf5 is essential for early embryogenesis and mammary gland development during pregnancy and lactation. *EMBO Journal*, *24*(3), 635–644.

8. Supplementary data

8.1. Oligonucleotide list

Name	Application	Sequence
hPBGD-1F	RT-qPCR	GGAGCCATGTCTGGTAACGG
hPBGD-1R	RT-qPCR	CCACGCGAATCACTCTCATCT
hELF5_iso2_CDS_F	RT-qPCR	TACTGGACTAAGCGCCATGT
hELF5_iso2_CDS_R	RT-qPCR	GCAGAAGGAGATGCAATTGG
hElf5_3UTR_F	RT-qPCR	GTGGAATGACAACAGCCCATGC
hElf5_3UTR_R	RT-qPCR	CATGCTTTCCCCCACCTTTGGT
hELF5-3xFlag_OX__F	RT-qPCR	TCGTCATCCTTGTAGTCGATGTCA
hELF5-3xFlag_OX__R	RT-qPCR	AAATGCACACGGGTGGCAGG
hTP63_F	RT-qPCR	AGAAACGAAGATCCCCAGATGA
hTP63_R	RT-qPCR	CTGTTGCTGTTGCCTGTACGTT
hTEAD4_F	RT-qPCR	CAGGTGGTGGAGAAAGTTGAGA
hTEAD4_R	RT-qPCR	GTGCTTGAGCTTGTGGATGAAG
hHLA-G_F	RT-qPCR	CCACCACCCTGTCTTTGACTAT
hHLA-G_R	RT-qPCR	ACGTCCTGGGTCTGGTCCT
hMMP2_F	RT-qPCR	TGGCACCCATTTACACCTACAC
hMMP2_R	RT-qPCR	ATGTCAGGAGAGGCCCCATAGA
hCGB_F	RT-qPCR	CAGCATCCTATCACCTCCTGGT
hCGB_R	RT-qPCR	CTGGAACATCTCCATCCTTGGT
hSDC1_F	RT-qPCR	CTATTCCCACGTCTCCAGAACC
hSDC1_R	RT-qPCR	GGACTACAGCCTCTCCCTCCTT
hGCM1-1F	RT-qPCR	GCTGGGACTTGAACCAGCAGT
hGCM1-1R	RT-qPCR	CTGGATCGGCCCACTCAAGC
hERVW-1_1F	RT-qPCR	CTACCCCAACTGCGGTTAAA
hERVW-1_1R	RT-qPCR	GGTTCCTTTGGCAGTATCCA

hElf5-insert-F	Cloning	GAGCTAGCATGTTGGACTCGG
hElf5-insert-R	Cloning	TGCTCGAGCCTAGCTTGT
hElf5_attB1_F	Gateway cloning	GGGGACAAGTTTGTACAAAAAAGCAGG CTTCACCATGTTGGACTCGGTGACAC
hElf5_attB2_R	Gateway cloning	GGGGACCACTTTGTACAAGAAAGCTGG GTTTTATAGCTTGTCTTCCTGCCACC
hELF5-V5_gt_1F	Genotyping	CCCAGAATTTCTCTTCTGCTTGCT
hELF5-V5_gt_1R	Genotyping	GGAGAGGGTTAGGGATAGGCTT
hELF5-V5_gt_2R	Genotyping	AGCTTGATGCCTGGAGCAGA
ELF5_EYFP_gt_1F	Genotyping	CACACGGGTGGCAGGAAG
ELF5_EYFP_gt_1R	Genotyping	CACCCTCCATAGACAACAACTCTGA
ELF5_EYFP_gt_2R	Genotyping	TCGTGCTGCTTCATGTGGTC
hELF5-V5_seq_1F	Sequencing	GGAGACAGTGTTTGTGTTCTG
hELF5-V5_seq_1R	Sequencing	CCTCCATAGACAACAACTCTG

8.2. shRNA list

Name	**shRNA ID**	**shRNA target sequence**	**Target**
shRNA-1	TRCN0000436380	AGTTCTCATCTATGGGAATTT	*ELF5* CDS
shRNA-2	TRCN0000431832	GACATTCGAAAGGCTTCATTT	*ELF5* 3'UTR
shRNA-3	TRCN0000013874	GCCCTGAGATACTACTATAAA	*ELF5* CDS

8.3. V5 knock-in components

Component	**Size**	**Sequence**
ELF5-specific crRNA sequence	20-mer	GACAAGCTATGATCTGCTCC
Left HA	75-mer	ATTTTGGAGCGGGTTGACCGAAGGTTAGTGTACAAATT TGGAAAAAATGCACACGGGTGGCAGGAAGACAAGCTA

Right HA	75-mer	TCTGCTCCAGGCATCAAGCTCATTTTATGGATTTCTGTCTTTTAAAACAATCAGATTGCAATAGACATTCGAAAG
V5 tag	42-mer	GGTAAGCCTATCCCTAACCCTCTCCTCGGTCTCGATTCTACG

8.4. Antibody list

Name	**Vendor**	**Catalog number**	**Application**	**Concentration**
Mouse IgG HRP-conjugated antibody	R&D	HAF008	WB	1:5000
Rabbit IgG HRP-conjugated antibody	R&D	HAF0018	WB	1:5000
Polyclonal rabbit Anti-CGB	Agilent	A023102-2	IF	1:250
Donkey anti-Rabbit IgG (H+L) Secondary Antibody, Alexa Fluor® 488 conjugate	Thermo Fisher Scientific	A-21206	IF	1:750
Donkey anti-Rabbit IgG (H+L) Secondary Antibody, Alexa Fluor® 594 conjugate	Thermo Fisher Scientific	A-21207	IF	1:750
Polyclonal rabbit Anti-ENDOU	Sigma-Aldrich	HPA067448	IF	1:200
Monoclonal Anti-FLAG M2	Sigma-Aldrich	F1804	IF	1:750

Monoclonal Anti-Lamin B1	Santa-Cruz Biotechnology	sc-374015	WB	1:750
Polyclonal Anti-ELF5	SZABO-SCANDIC	SACSC-9645	WB	1:750
Polyclonal rabbit Anti-ELF5	Thermo Fisher Scientific	720380	IF	1:250